An Investigation into Ultrasonic Communication for Near-Body Networks

By

Eric Joshua Escudero & Gursewak Singh Rai

Senior Project

ELECTRICAL ENGINEERING DEPARTMENT

California Polytechnic State University

San Luis Obispo

June, 2011

TABLE OF CONTENTS

Section   *Page*

LIST OF TABLES AND FIGURES

ACKNOWLEDGEMENTS

ABSTRACT

The following report presents a study of body-area, free-space ultrasonic communication system. Two analog communication systems are investigated. The initial communications system setup relies upon the amplitude modulation (AM) techniques to transmit the signal. Such a system is prone to noise since the amplitude of the signal is directly affected by distance and the signal strength will deteriorate. The secondary communication system involves utilizing frequency modulation (FM). This method avoids the issue of losing information due to amplitude deterioration, but encounters delay issues. The main hardware components used in the approach outlined include ultrasonic transducers (UTs) used for both transmitting (Tx) and receiving (Rx), modulation and demodulation stages, several filters, an audio microphone and amplifier, and a speaker. The range of interest is 1-2 meters compared to radio frequency (RF) communication ranges of kilometers. For medical use, this range need not exceed a human's body length.

I.   INTRODUCTION

In the medical profession, doctors commonly measure a variety of vitals including blood sugar content, blood pressure, and heart rate of long-term patients. In many cases, patients are hooked up to several machines in order to monitor these vitals. A better technique would be to "MUX" together this data and wirelessly send it to a monitoring system. Although various RF communication methods exist, such as Bluetooth and Zigbee, a significant amount of power is consumed by these systems. Typically, a Class 2 Bluetooth device will consume 2.5 mW in the range of ten meters and a Class 3 device will consume 1 mW within 1 meter [1], which is similar for a Zigbee device. RF communications also have the downsides in regards to health. They emit high frequency radiation which can penetrate through skin and have adverse health effects [2]. Since the data rate required to monitor the aforementioned vitals is low (typically a few kpbs), ultrasonic communication represents an alternative approach to traditional RF methods. This paper presents a prototype that, with refinement, may be used in the application described above or in any other application that requires low-rate, low-power, and short distance communication systems.

II.   BACKGROUND

2.1 Importance of Ultrasonic Communication

Ultrasonic communication is often considered inferior to radio and microwave communications due to its short range and low bandwidth. Radio and microwave communications are used in a wide variety of applications such as AM and FM radio, television broadcasting, and electronic warfare systems. Although radio and microwave communications encompass a wider variety of applications than ultrasonic communications, they cannot be utilized in various near-body applications due to the high exposure of radiation, which even in relatively small amounts can cause irreparable damage to cells and tissues. Along with serving as a means of navigation, communication and defensive mechanisms for many species in nature, ultrasonic communication provides advantageous qualities for many applications in the medical field due to its low-risk of radiation damage to cells. Therefore, this paper will investigate the use of ultrasonic communication for near-body applications.

2.2 Piezoelectric Effect

This paper investigates the use of UTs as transmitters and receivers in a communication system. A UT converts electrical energy into sound waves (and vice versa) in the ultrasonic range, which refers to sound frequencies not perceived by human hearing (above 20 kHz). This type of transducer takes advantage of a process referred to as the piezoelectric effect in which a voltage is generated when mechanical strain is induced on a piezoelectric material, or vice-versa. See Figure 1 for illustration. The piezoelectric materials that are required for this effect to occur must be non-conductive

and belong to one of two main groups, crystals (most well-known is the quartz crystal) and ceramics.
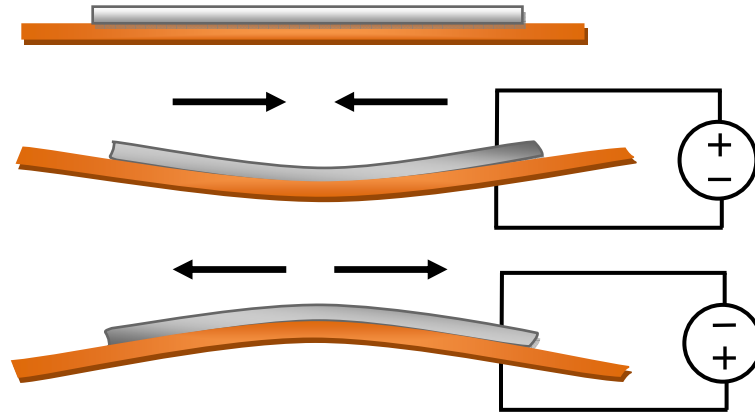
Figure 1: *Piezoelectric effect on a non-conductive material*

The piezoelectric effect occurs due to the concentration of electric dipole moments in solids. A piezoelectric material has a high dipole density. This effect arises from the polarization of an electric field in the material $\left(\vec{D} = \varepsilon\vec{E}\right)$, and Hooke's law $(\vec{S} = s\vec{T})$, which in turn relates the strain to the stress on a material [3-4]. Strain changes the permittivity of the material which affects the electric field and essentially the induced electromotive force. Ultimately, sound waves are emitted at frequencies corresponding to that of the alternating voltage applied to the transducer.

2.3 The Need for Modulation

Multiple factors must be considered before designing a wireless communication system. Some of these limiting factors include the type of signal to be sent, the distance at which the signal is required to travel, the bandwidth of the signal and antenna size. Modulation techniques are necessary in communication systems because of their advantageous qualities in regards to these factors. For efficient radiation of an

electromagnetic (EM) or acoustic wave, the radiator (i.e. antenna, UT, etc.) must be comparable in size to the largest transmitted wavelength. This corresponds to the equation, $\left(\lambda = \frac{v}{f}\right)$, where v is the wave velocity, f is the frequency, and λ is the wavelength. Thus, a smaller frequency requires a larger antenna size. Modulation techniques minimize the necessary antenna size by superimposing the desired band of frequencies, which is the message frequency (such as 1-4 kHz tone in this case), onto another band of frequencies, known as the carrier frequency (40 kHz in this case) with minimal distortion [5]. These techniques also take advantage of the improved propagation characteristics of higher frequency EM and acoustic waves in air, along with efficiently utilizing the EM spectrum due to its effect on the bandwidth of the transmitted signal.

There are many modulation techniques in use today, with digital modulation techniques becoming more common in an increasingly wide variety of applications. Even though digital modulation contains higher efficiency than analog modulation, it involves highly complex circuitry and concepts, such as error correction. In any development process, such as this one, it is important to start off experimenting with a simpler system to understand the underlying issues. Therefore, analog AM and FM techniques are investigated in this project and only the demodulation circuitry for each technique is designed and constructed.

2.4 Demodulation

Once a signal is modulated and sent over a wireless link, a receiver system must contain a demodulation stage in order to retrieve the desired message signal. There are

multiple techniques that can be used to demodulate a received signal. Simple

demodulation techniques that are explored in this project include AM and FM

demodulation.

2.4.1 AM Demodulation

The circuitry for a simple AM receiver system includes a full-wave rectifier, a

low-pass filter, and a DC block stage. This system, excluding the DC block stage, is also

referred to as an envelope detector. A block diagram of the AM receiver system is

illustrated in Figure 2.

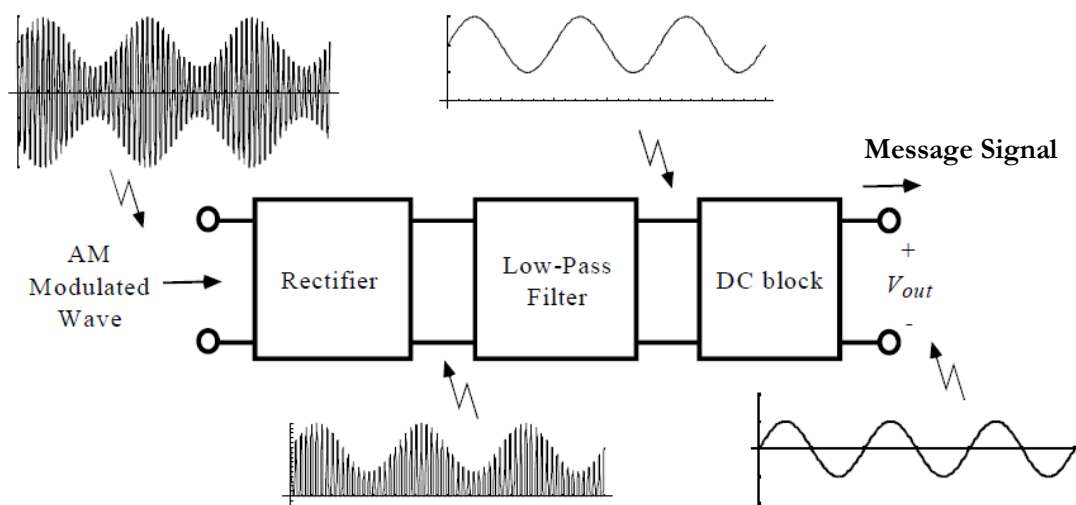**Figure 2:** *Block diagram of a simple envelope detector system [6]*

Once the modulated signal is transmitted, the full-wave rectifier is responsible

for rectifying the received signal (i.e. obtaining the absolute value of the modulated

signal). This results in a signal with positive pulses of varying magnitudes at the carrier

frequency. Next, a low-pass filter is used to remove the carrier frequency and retrieve the

message signal. After filtering, the retrieved signal contains a DC offset, which is easily

removed by using a DC block – essentially, a coupling capacitor.

2.4.2 FM Demodulation

The following equation describes modulation of a message signal at a carrier

frequency.

$$x_{FM}(t) = A_c \cos\left[2\pi f_c t + \frac{f_\Delta}{f_m}\cos(2\pi f_m t)\right]$$ (1)

$A_c \equiv$ The amplitude of the carrier
$f_c \equiv$ The frequency of the carrier
$f_\Delta \equiv$ The frequency deviation
$f_m \equiv$ The frequency of the message signal

The term $\frac{f_\Delta}{f_m}$ refers to the maximum shift away from the carrier frequency. So, it

can be inferred that the frequency deviation should be on the order of f_m. If the

frequency deviation is too small, there will be under-modulation and the signal will not

be intelligible when demodulating. Distortion results if the frequency deviation is too

large. Since the message information resides in the instantaneous frequency of an FM

waveform, a frequency-selective network is required to yield an output proportional to

the instantaneous frequency. An illustration of this process is in Figure 3a. The simplest

method to perform this operation is by utilizing a differentiator. Figure 3b shows the

resulting output of a differentiator due to an FM modulated input waveform. The output

of the differentiator could then be passed through the envelope detector discussed in the

above AM demodulation section to obtain the message signal. This method is

investigated in this project.
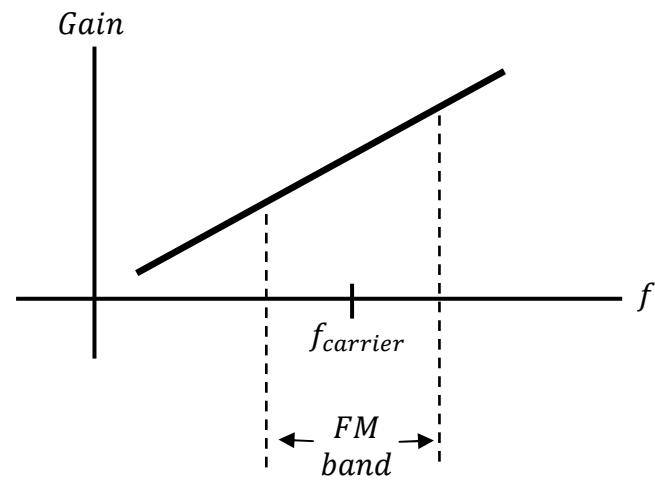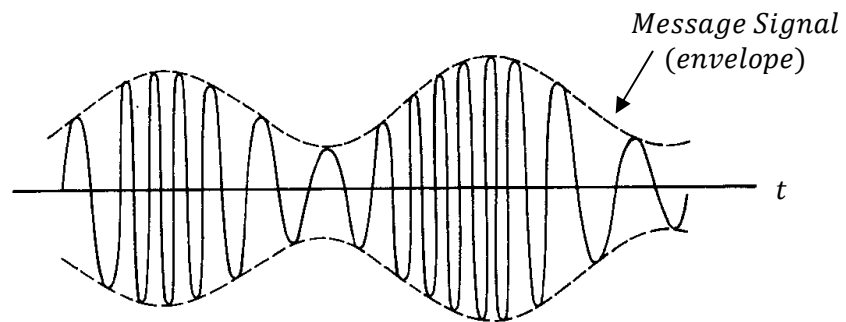
Figure 3: *(a) Ideal FM demodulator frequency response*
(b) Output of a differentiator with an FM input waveform

III. REQUIREMENTS

The main goal of this project is to first investigate the performance of UTs within a range of 1-2 meters and also assess the performance of various analog modulation techniques within an ultrasonic transceiver system. In order to obtain a census on which methods are optimal for future investigation of a digital ultrasonic system, multiple objectives must be met:

1)   Analyze the performance of various UTs to be used for transmitting and receiving the desired signal.

2)   Develop demodulation circuits for both AM and FM cases

3)   Analyze overall performance for each case (parameters include power consumption, size, desired Tx-Rx distance, and feasibility).

IV. DESIGN

4.1 Overview of Ultrasonic System

This project only encompasses the design of the demodulation circuitry for an ultrasonic communication system. The two demodulation circuits that will be explored include AM and FM techniques. A complete block diagram of the system is illustrated in Figure 4. The "switches" represent the individual paths for the AM and FM systems.
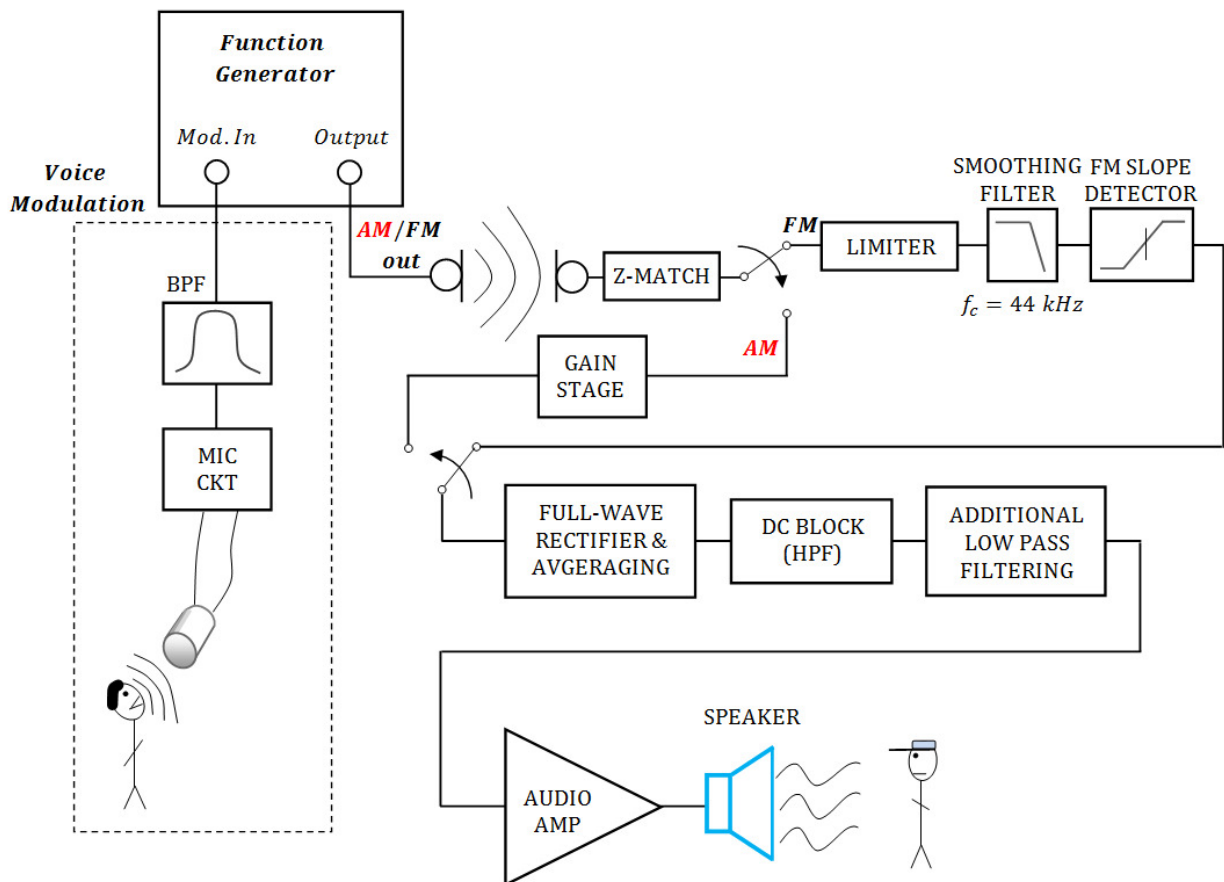

Figure 4: *Block diagram of AM and FM demodulation systems*

A sinusoidal tone signal at frequency of 1 kHz is superimposed with a carrier frequency of 40 kHz with equal amplitude. This modulated signal, created internally via

the function generator, is transmitted through the Tx UT and received via the Rx UT (see Integration and Testing for more information regarding the impedance matching block after the Rx UT). Depending on if the signal is AM or FM, the system is configured as shown in Figure 4. The gain stage is utilized to amplify the signal to greater amplitudes for the case of an AM input waveform. In the case of an FM input waveform, the limiter plays the role of setting the waveform to a certain peak-to-peak voltage level (in the case of this project, the supply voltage rails). The FM signal is sent through a limiter, smoothing filter, and slope detector, before reaching the full-wave rectifier circuit. For AM, the signal is sent directly to the full-wave rectifier circuit. At this point, the AM and FM cases share the remaining circuitry. The rectified waveform contains a DC offset that is removed using a DC block circuit (capacitor coupling). Additional low-pass filtering is used before amplifying the demodulated signal via an audio amplifier and sending to a speaker for verification.

4.2 Ultrasonic Transducer (UT) Selection

There are numerous types of UTs available in today's market. Therefore, a reasonable amount of time was designated to finding an optimal UT for the particular project at hand. Some key characteristics that were considered during the selection process of an appropriate UT include bandwidth, driving voltage, directivity, sensitivity, nominal output impedance, size, and cost. The most important considerations were size and power. Since an application for this UT would be to integrate within a portable device, such as a watch, wrist strap, etc., a small UT with a wide radiation pattern and

low power consumption is optimal. Therefore, the size and sensitivity led to the selection

of the Knowles Acoustic SPM0404UD5 UT, which is illustrated in Figure 5.
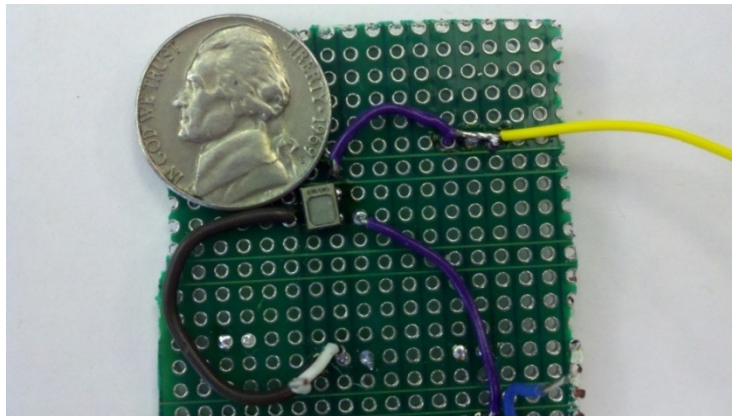
Figure 5: *Size comparison of UT (Knowles Acoustic: SPM0404UD5)*

Other UTs considered include the Kobitone (#255-400ST12-ROX), illustrated

in Figure 6, and the ceramic disc UT by Steminc (SMD07T02R412WL) illustrated in

Figure 7. These UTs were chosen upon reviewing their sensitivity, bandwidth, and center

frequency at the chosen operating frequency of 40 kHz +/- 1 kHz. A list of some of the

electrical characteristics for various UTs that were considered is illustrated in Table 1.

Figure 6: *Size comparison of UT (Kobitone #255-400ST12-ROX)*
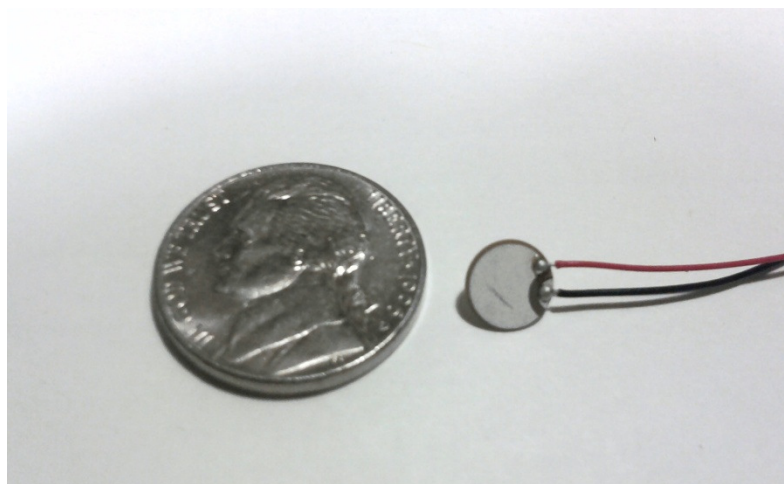
Figure 7: *Size comparison of UT (Steminc SMD07T02R412WL)*

Table 1: *Ultrasonic transducer electrical characteristics*

Ultrasonic Transducer	Maximum Driving Voltage	Center Frequency (@ f_0)	Nominal Output Impedance	Bandwidth	Beam Angle (@ -6 dB)	Sensitivity (@ f_0)
Kobitone: #255-400ST12-ROX	20 V_{p-p}	40.0 kHz +/- 1.0 kHz	N/A	2 kHz (@ -6 dB)	N/A	-67 dB (0dB=1V/μbar)
Kobitone: #255-400PT16- ROX	20 V_{p-p}	40.0 kHz +/- 1.0 kHz	1,000 Ω	2 kHz (@ -6 dB)	55°	-53 dB
Kobitone: #255-400ST16- ROX	20 V_{p-p}	40.0 kHz +/- 1.0 kHz	N/A	2.5 kHz (@ -6 dB)	N/A	-65 dB
Kobitone: #255-400ER25- ROX	20 V_{p-p}	40.0 kHz +/- 1.0 kHz	N/A	1 kHz (@ -6 dB)	N/A	-70 dB
Knowles Acoustics: SPM0404UD5	3.6 V (DC)	45 kHz +/- 15.0 kHz	300 Ω	30 kHz	N/A	10 dBV/Pa

4.3 Gain Stage (AM Only)

For the AM case, a gain stage is connected directly after the impedance matching and high pass filtering network of the Rx UT. This gain stage is used to amplify the received signal. Figure 8 illustrates the non-inverting op-amp-based circuit configuration designed to create the gain stage.
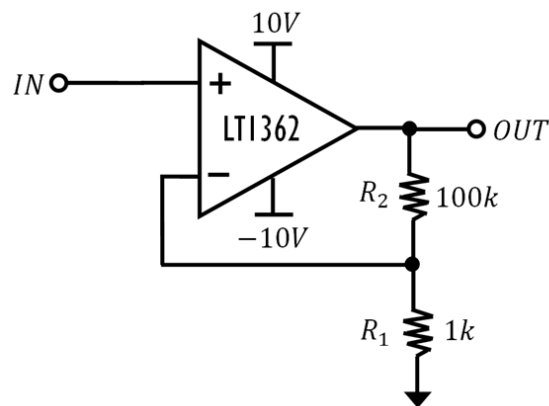
Figure 8: *Non-inverting op-amp-based gain stage circuit schematic*

A gain of 101 V/V was created using resistor values of 1 kΩ for R$_1$ and 100 kΩ for R$_2$. The gain stage is needed to amplify the signal since an input signal of $1V_{p-p}$ is applied via the function generator and the distance between the UTs deteriorates the amplitude of the transmitted signal. The LT1362 Op-Amp IC package is chosen for all circuits needing an op-amp since it contains an appealing gain-bandwidth product of 50MHz.

4.4 Limiter (FM Only)

For the FM case, a limiter is designed using the LM339 Quad-Comparator IC package and located directly following the impedance matching network. This limiter is

utilized in the system to allow signals with amplitudes below a specified voltage to be boosted to a certain voltage level and attenuate the peaks of stronger signals that exceed this level. This essentially reduces the effects in variations that the input signal level has on the output. The limiter circuit configuration is illustrated in Figure 9.
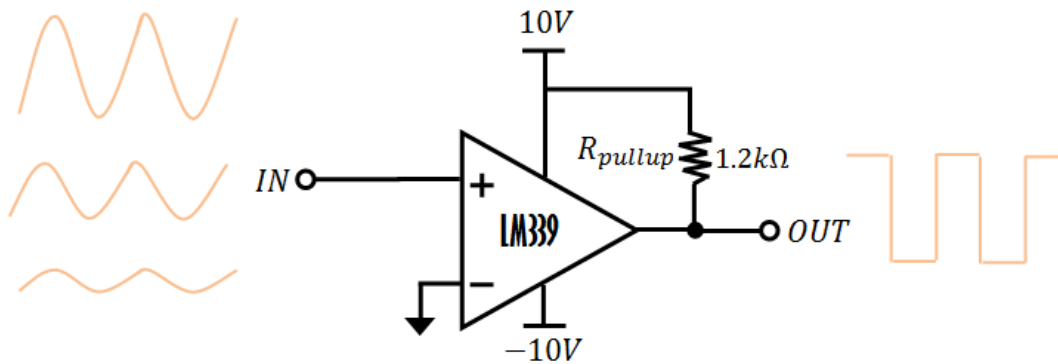
Figure 9: *Limiter circuit schematic*

In this case, a simple implementation of a limiter is designed with one comparator from the LM339 package and a pull-up resistor of 1.2 kΩ, which allows for switching between the positive and negative rails. The negative terminal is chosen to be the reference level at ground potential. The sinusoidal input signal is essentially transformed into a square waveform signal with amplitude of 20 V$_{p-p}$, which is the range of the supply voltage.

4.5 Smoothing Filter (FM Only)

The output signal of the limiter is essentially a square waveform. However, a sinusoidal waveform is desired because the carrier signal is of the same form and this will result in better demodulation of the signal. Therefore, a smoothing filter is used following the limiter in order to transform the signal back to a sinusoidal waveform. A

circuit configuration of the smoothing filter designed using TI's *FilterPro* is illustrated in Figure 10.
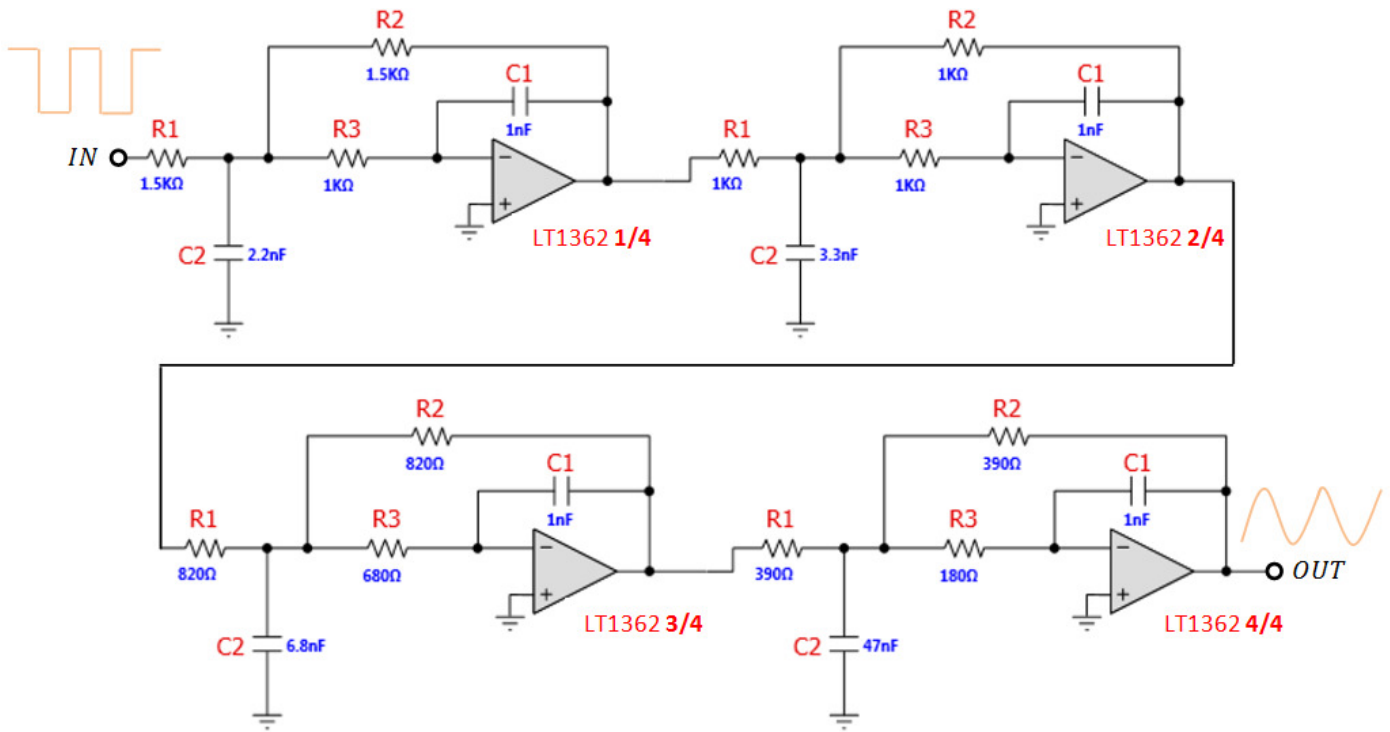
Figure 10: 8th *order low-pass filter circuit schematic*

A square waveform can be represented using the Fourier Series, which is essentially a sum of infinite sinusoidal waveforms as shown in Equation 2. Even though the output of the limiter is not an ideal square waveform, the same analysis may be used. Essentially, a square wave is made up of odd harmonics as illustrated in Equation 2.

$$x_{square}(t) = \frac{4}{\pi} \sum_{k=1}^{\infty} \frac{\sin[(2k-1)2\pi ft]}{(2k-1)}$$
$$= \frac{4}{\pi} \left[\sin(2\pi ft) + \frac{1}{3}\sin(6\pi ft) + \frac{1}{5}\sin(10\pi ft) + \cdots \right]$$

(2)

Upon designing the smoothing filter, the frequency range of interest needs to be considered. With a frequency deviation of 4 kHz, as well as a maximum input frequency

also at 4 kHz, and a carrier frequency of 40 kHz, the resulting frequency range for the smoothing filter is 40 kHz +/- 4 kHz (36 kHz to 44 kHz). Therefore, frequencies falling within this range will pass without attenuation while higher order odd harmonics are attenuated. In the worst case of a 36 kHz sinusoidal wave, the 3rd harmonic is 108 kHz has the greatest effect on the signal. Applying these restrictions within *FilterPro*, an 8th order low-pass filter (cutoff frequency at 85 kHz) of the Butterworth response using a multiple-feedback topology was created. The multiple-feedback topology was selected due to its lower sensitivity to component variation.

4.6 FM Slope Detector (FM Only)

There are various methods in performing an FM slope detector, which is essential in the FM demodulation circuit. The simple approach of using a high-pass filter with an appropriately selected cutoff frequency was taken in this project to perform this task. A circuit configuration of the high-pass filter is illustrated in Figure 11.
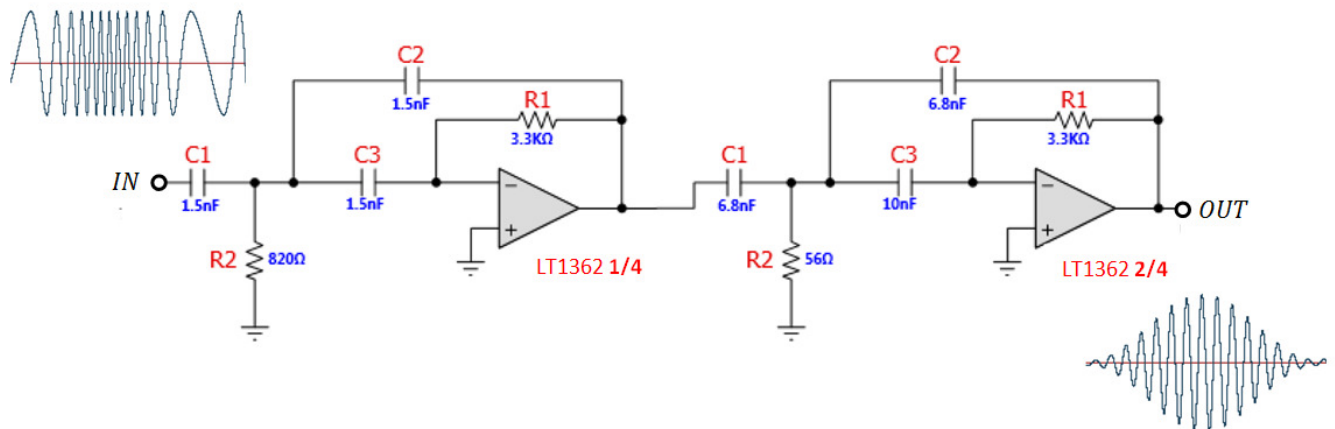

Figure 11: *4th order high-pass filter circuit schematic*

This circuit, which was created using *FilterPro*, will essentially convert FM to AM through varying the attenuation of the amplitude in relation to the frequency of the input signal. The difference between the attenuation of an input signal at the lowest frequency (in this case 36 kHz) and at the highest input frequency (44 kHz) depends on the roll-off slope of the high-pass filter. The higher the order, the greater the roll-off which results in a greater difference in attenuation at the two frequencies. For illustration of this process, see Figure 3a. The designed filter was chosen to be a 4th order high-pass filter with a multiple-feedback topology and a 0.5 dB Chebyshev response type. This response type was chosen for its faster roll-off slope compared to the Butterworth response type. This is important because the operating frequency range of interest (36 kHz to 44 kHz) must have a linear relationship between the output voltage and the input frequency. The cutoff frequency was chosen to be 45 kHz since the filter simulation showed a nearly-linear and steep response for the range of interest and the overall attenuation was not excessive.

4.7 Envelope Detector

The envelope detector is a circuit common to AM and FM demodulation. In this project, this circuit is directly responsible for demodulating the AM waveform, which is produced in both the AM and FM cases. The approach taken to implement the envelope detector involves a full-wave rectifier and an active low-pass filter. This circuit is illustrated in Figure 12.
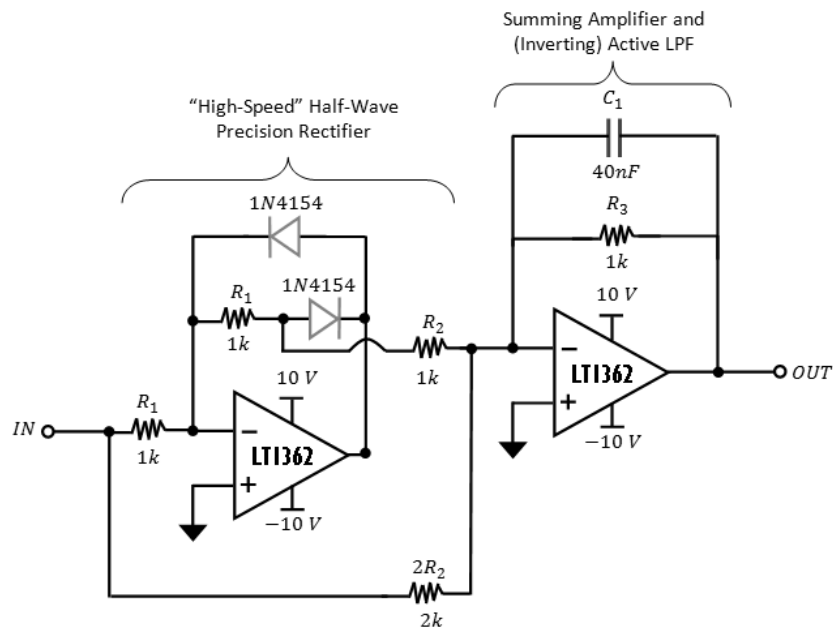
Figure 12: *Envelope detector circuit schematic [7]*

After being amplitude modulated, the signal is sent to a "high-speed" half-wave rectifier stage that contains one op-amp from the LT1362 IC package, two 1 kΩ resistors and two 1N4154 diodes. This precision rectifier allows current to flow through the resistor and diode branch during positive voltage excursions. Ideally, a voltage drop of approximately 0.7 V is experienced across the conducting diode when forward biased which creates an inverted signal of nearly zero gain during these positive voltage cycles. When on negative voltage cycles, the current flows through the feedback diode, resulting in zero potential at the output. This creates a "high-speed" half-wave precision rectifier compared to a "low-speed" circuit configuration, one without a feedback [7].

The next stage consists of a summing amplifier with an active low-pass filter connected in the feedback. When cascaded to the half-wave rectifier, the result is an absolute value of the input signal with a gain of the ratio of R_3/R_2. This is due to the fact

that the first branch to the summing amplifier contains half the resistance of that in the

second branch, which allows twice the current to flow in the first branch and half the

steepness in the transfer function characteristics of the second branch [7]. Therefore,

when summing the two signals together, the resulting output signal is entirely rectified

and inverted compared to the input signal. The active low-pass filter consists of a

capacitor across the feedback resistor in the second stage of Figure 12. Using Equation

3, with (R=R_3, C=C_1 from Figure 12) the 3dB frequency cutoff is calculated to be 3.979

kHz, which successfully filters out the carrier frequency of 40 kHz and retrieves the

desired message signal.

$$f_{3dB} = \frac{1}{2\pi RC}$$
(3)

4.8 DC Block Stage

Once the signal is completely rectified and the carrier frequency of 40 kHz is

filtered out, the signal will contains a DC offset. The next stage consists of a circuit that

eliminates this DC offset using a 2nd order high-pass filter configuration. This circuit is
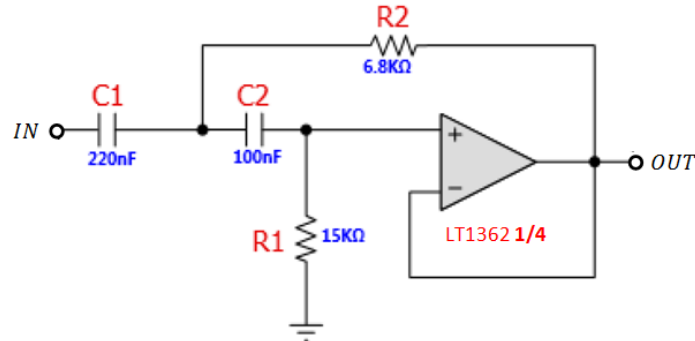
illustrated in Figure 13.

Figure 13: *2ⁿᵈ order high-pass filter circuit schematic*

Even though removing the DC offset could ideally be executed using only a capacitor, a high-pass filter was chosen to implement this operation in order to also filter out low frequency noise. The 2ⁿᵈ order filter was designed using *FilterPro* and uses a Sallen-Key topology with a Butterworth response type. The cutoff frequency was chosen to be at 100 Hz because frequencies lower than about 300 Hz are insignificant in human speech, which will be used as a message signal.

4.9 Additional Filtering

An additional 4ᵗʰ order low-pass filter circuit is utilized to remove any further high frequency harmonics that is left over from the rectifier stage. This circuit is illustrated in Figure 14.
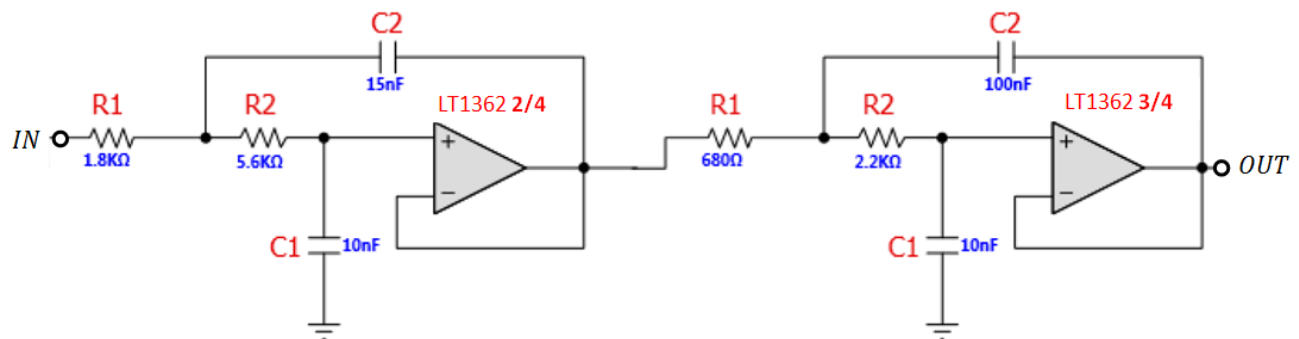
Figure 14: *4th order low-pass filter circuit schematic*

This 4th order low-pass filter circuit was designed using *FilterPro* and contains a Sallen-Key topology with a Butterworth response type. The chosen cutoff frequency is 4kHz, which allows the projected 1 kHz to 4 kHz tone frequencies to pass through while attenuating higher frequencies.

4.10 Audio Amplifier

The message signal that is retrieved after this process is then sent to an audio amplifier followed by a speaker for verification. The audio amplifier circuit that was utilized is illustrated in Figure 15. This circuit was borrowed from the LM386 datasheet.
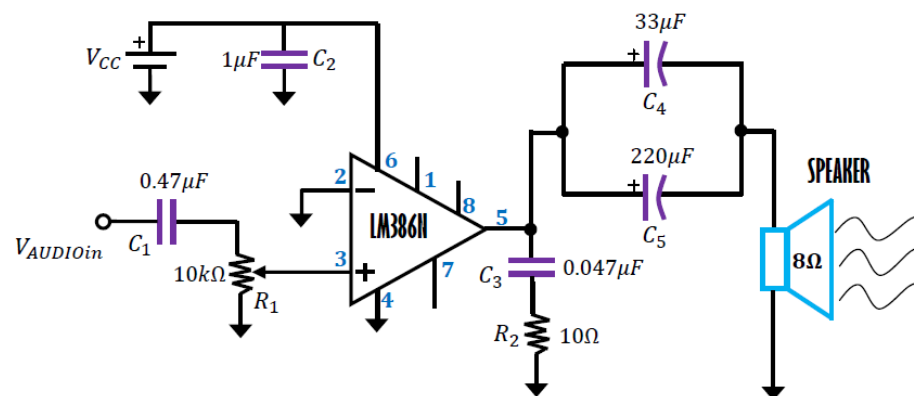

Figure 15: *Audio amplifier circuit schematic*

4.11 Microphone Circuit

In this project, the transmission of voice through the communication channel is performed as another measure of the performance of the communication system. In order to transmit a voice signal, a microphone and interface circuitry is needed. The microphone used in this circuit is a condenser microphone. A condenser microphone exploits electrostatic forces instead of magnetic inductance. It is basically a variable capacitor whose capacitance varies with sound. This is achieved by allowing one of the capacitor's plates to have mobility. When the capacitor's static plate is charged and the mobile plate oscillates due to an incoming sound wave, the voltage across it will vary. The condenser microphone is biased with a resistor as seen in Figure 16. When the voltage across the capacitor varies, the current through the resistor varies and changes the output current.

$$C = \varepsilon_r \varepsilon_o \frac{A}{d} \tag{4}$$

$A \equiv$ Area of overlap of the two plates remains constant
$\varepsilon_r \equiv$ Relative static permittivity
$\varepsilon_r \equiv$ Electric constant
$d \equiv$ Separation between plates

$$C = \frac{Q}{V} \quad \rightarrow \quad V = \frac{Q}{C} \tag{5}$$

$Q \equiv$ Electric charge
$C \equiv$ Capacitance
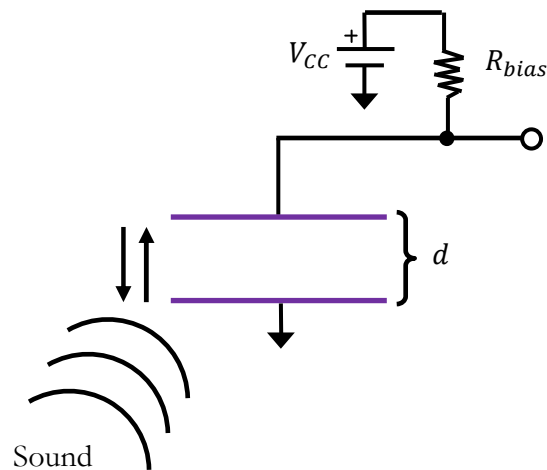$V \equiv$ Voltage potential

Figure 16: *Equivalent circuit of a biased condenser microphone*

The circuit in Figure 17 illustrates a biased microphone, cascade gain and low-pass filtering stage. The capacitor following the biasing circuit allows only changing voltages to pass across the capacitor. The gain stage allows for a variable gain up to a maximum of about 9 V/V. The low-pass filter type is a 2nd Order Butterworth response with a Sallen-Key topology and was designed using *FilterPro*. The cutoff frequency is 4.5kHz, which results in the rejection of frequencies outside the bandwidth of the transmitter. The op-amp types used were LM741.
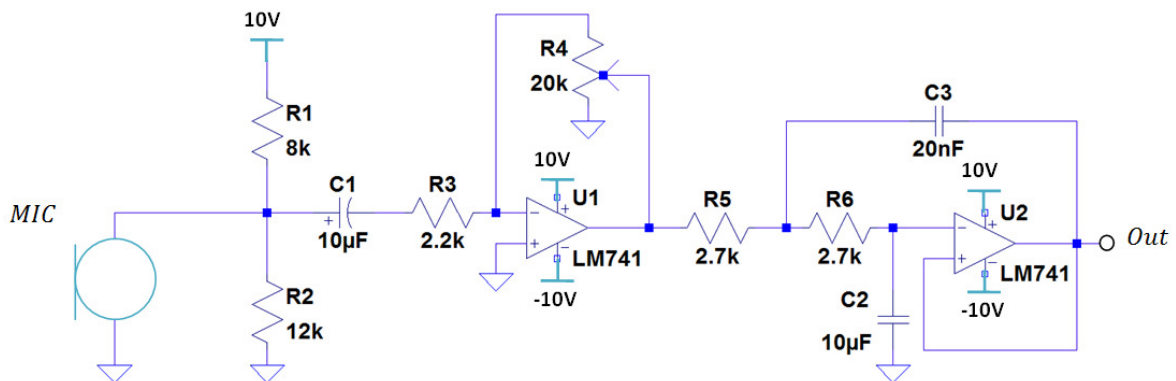

Figure 17: *MIC circuit schematic*

V. INTEGRATION AND TEST RESULTS

5.1 Ultrasonic Transducer Characterization

One of the main goals of this project is to find and characterize the UTs that are to be utilized as a transmitter and receiver for the ultrasonic system. An ideal UT would be capable of both transmitting and receiving. However, this is not the case for all UTs. Thus, due to the lack of information on various datasheets for these UTs, a reasonable amount of time was spent testing and characterizing them in order to determine if any one of them could be utilized as both a transmitter and receiver.

Initially, a pair of the UTs (Knowles Acoustic: SPM0404UD5) were tested without any amplification, but with no received signal, an amplifying stage was added as illustrated in the circuit in Figure 18.
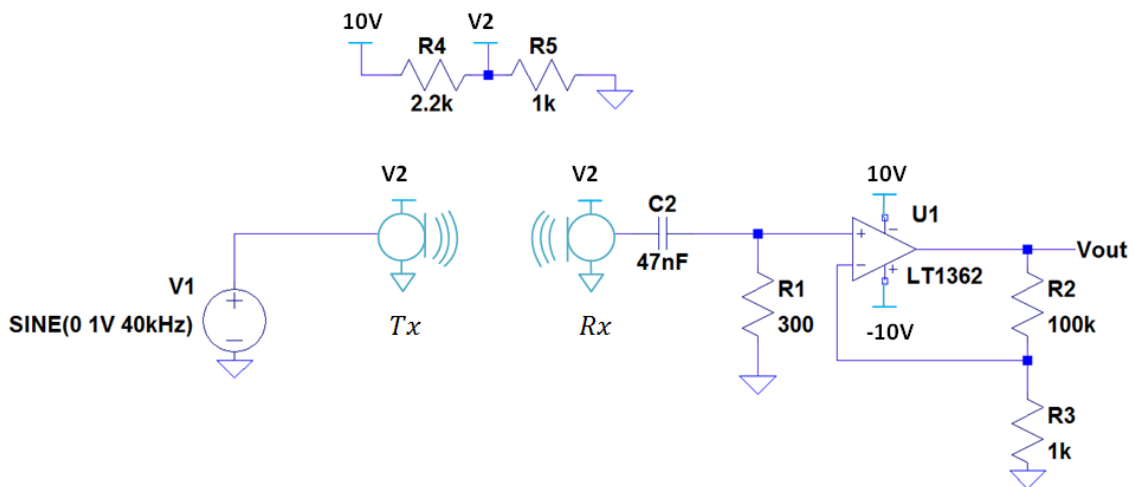

Figure 18: *UT characterization test circuit schematic*

The received signal is first high-pass filtered using a capacitor of 47 nF and resistor value of 300 Ω to achieve a cutoff frequency of 11.3 kHz. The resultant waveforms were distorted (i.e. the signal did not contain a purely sinusoidal wave). This

proved to be a false positive after varying the distance between the UTs and not obtaining any variance in the received signal. Therefore, it was determined that the SPM0404UD5 UT is incapable of transmitting. Other UT pairs were tested in the same manner. After experimenting with various pairs and combinations of the UTs listed in Table 1, it was determined that the optimal combination involved the Kobitone #255-400ST12-ROX as the transmitter (due to its wide beam angle pattern and size) and the Knowles Acoustic SPM0404UD5 as the receiver (due to its receiving sensitivity range and size). In order to characterize the selected UT pair, measurements of the peak-to-peak voltage versus the distance from the transmitter to the receiver were obtained using the circuit illustrated in Figure 18, with a change made to the Tx biasing.

A plot of the voltage versus the distance between various UTs is illustrated in Figure 19. This data was taken at an operating frequency of 40 kHz and an input voltage of 1 V_{p-p}. The plot demonstrates how the magnitude of the transmitted signal decreases with distance. The magnitude drops with a 1/r relationship similar to propagating electromagnetic waves (with r equal to the distance between the Tx and Rx UTs). Note that the distance measurements for the Kobitone #255-400ST12-ROX UT starts at 0.36 meters; this is due to saturation of the signal for closer distances. At smaller input voltages, the curve will follow the same pattern.
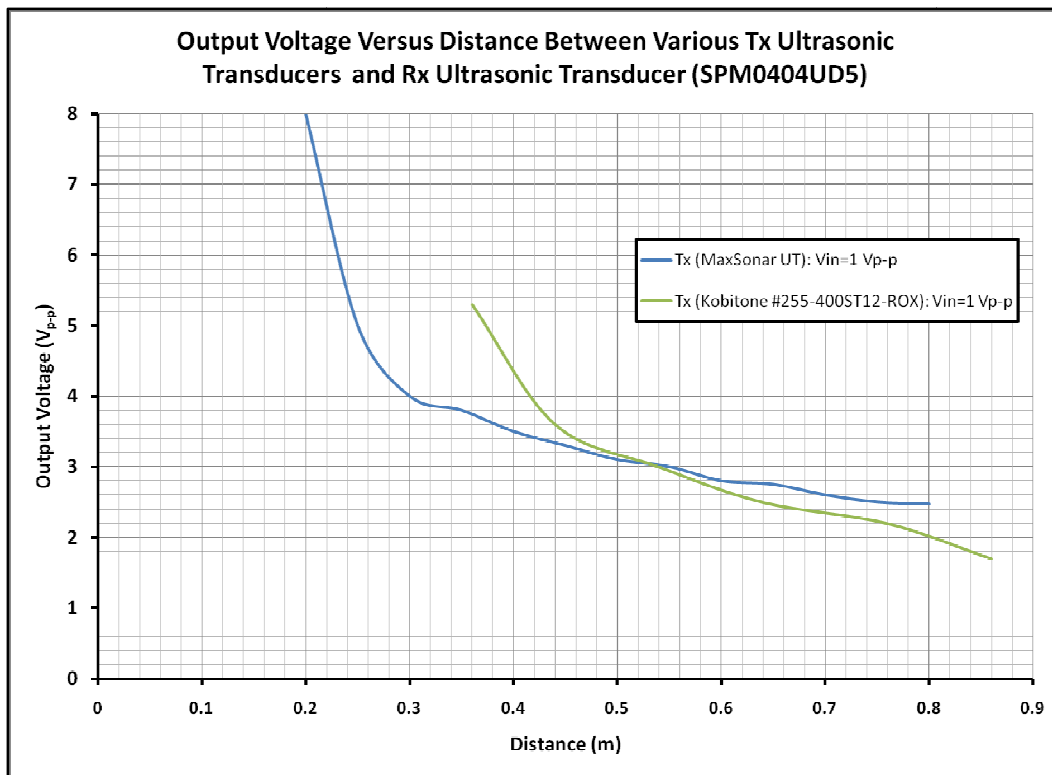
Output Voltage Versus Distance Between Various Tx Ultrasonic Transducers and Rx Ultrasonic Transducer (SPM0404UD5)

Figure 18: *Plot of voltage versus distance for Tx-Rx UT system*

A plot of the power consumption as a function of the input peak-to-peak voltage was taken for the Tx UT and is illustrated in Figure 20. This plot demonstrates sub-mW power consumption up to 5 V_{p-p}. This characteristic is particularly important for the purpose of this project because the power consumed is less than 1 mW for the operating voltage range of interest. Particularly, at 1 V_{p-p}, the power consumption is about 24 µW.
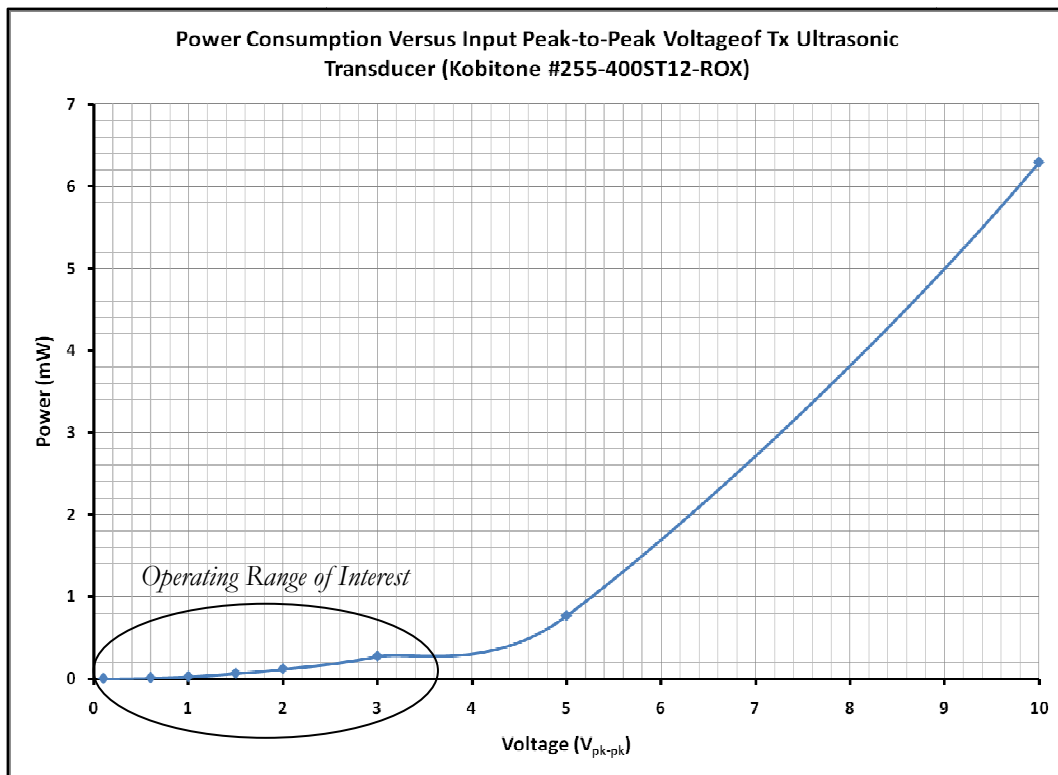
Figure 19: *Plot of power consumption versus input voltage for Tx UT*

Figure 21 illustrates the method taken to determine the radiation pattern of the UT system. A microphone stand was utilized to fix the height at about 0.74 meters. The neck of the stand held the Tx UT and was rotated as shown in Figure 21 to obtain the radiation pattern illustrated in Figure 22. Note that the Rx UT was stationary and located directly beneath the Tx UT.
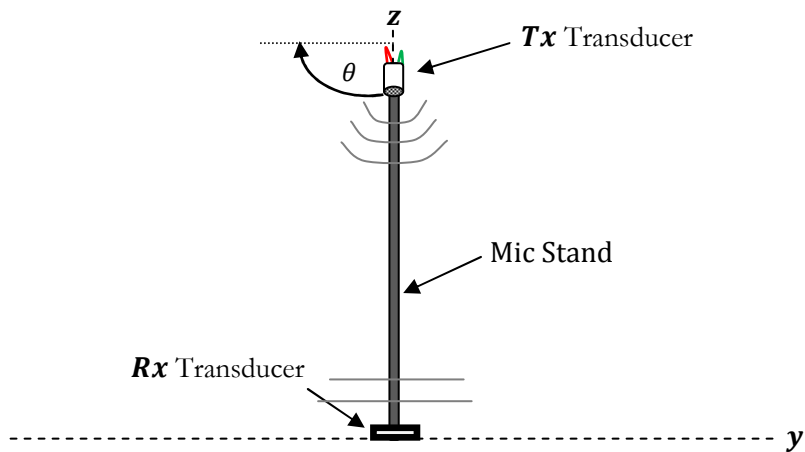
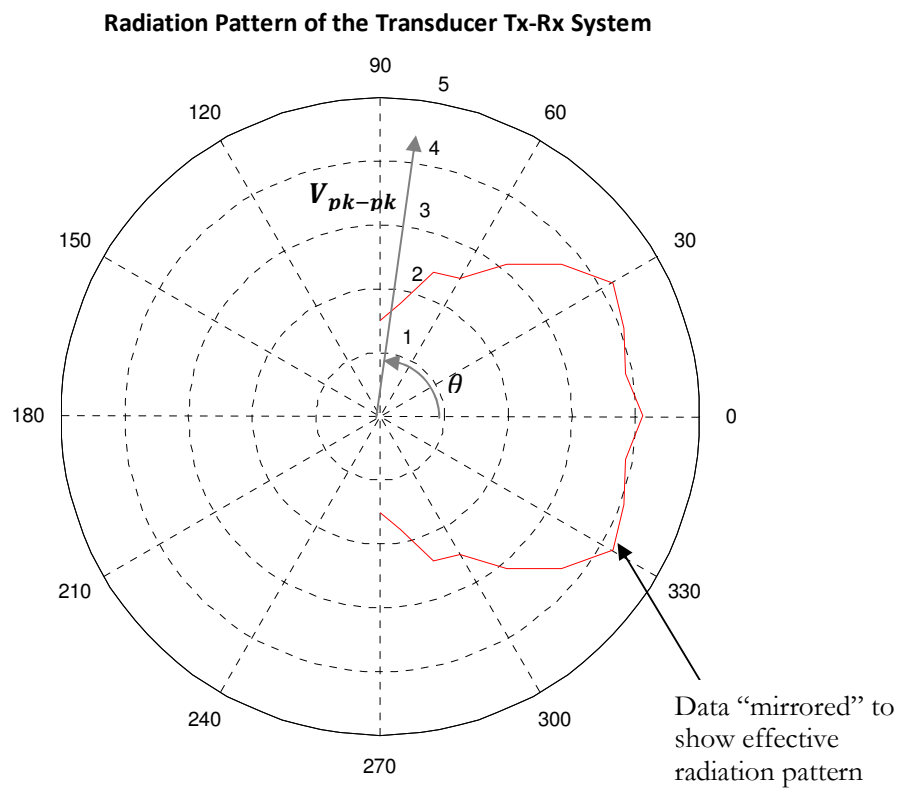**Figure 20:** *Testing configuration for radiation pattern (y-z cross section)*

Figure 21: *Radiation pattern of Tx-Rx UT system*

This radiation pattern shows a wide beamwidth with least radiation at 90° with respect to the Rx UT. The wide beamwidth is appealing since reception can be achieved at many different angles. In terms of angles greater than 90°, reception may be possible through multipath reflections. It can be related to two people of having a conversation; in the vicinity, their conversation is heard, but at a greater distance away their voices become distorted. In the case of this project, the communication channel is within 1-2 meters, a reasonable distance for sound waves to traverse.

5.2 Limiter Performance

The limiter circuit performance is illustrated in Figure 23. A 2 V_{p-p} sinusoidal wave is applied to the input. The output of the limiter is a square waveform at 20 V_{p-p}. For this project, the performance of the limiter at this input voltage range contains relatively efficient transitions around the rising and falling edges of the square waveform compared to lower input voltages. Figure 24 illustrates how the limiter's performance begins to break down when a low enough input voltage is applied; in this case, the limiter can sense roughly 4 mV_{p-p}, with some distortion. In this circuit, the distortion is not a major issue since a smoothing filter follows the limiter to reproduce a smoother sinusoidal wave.
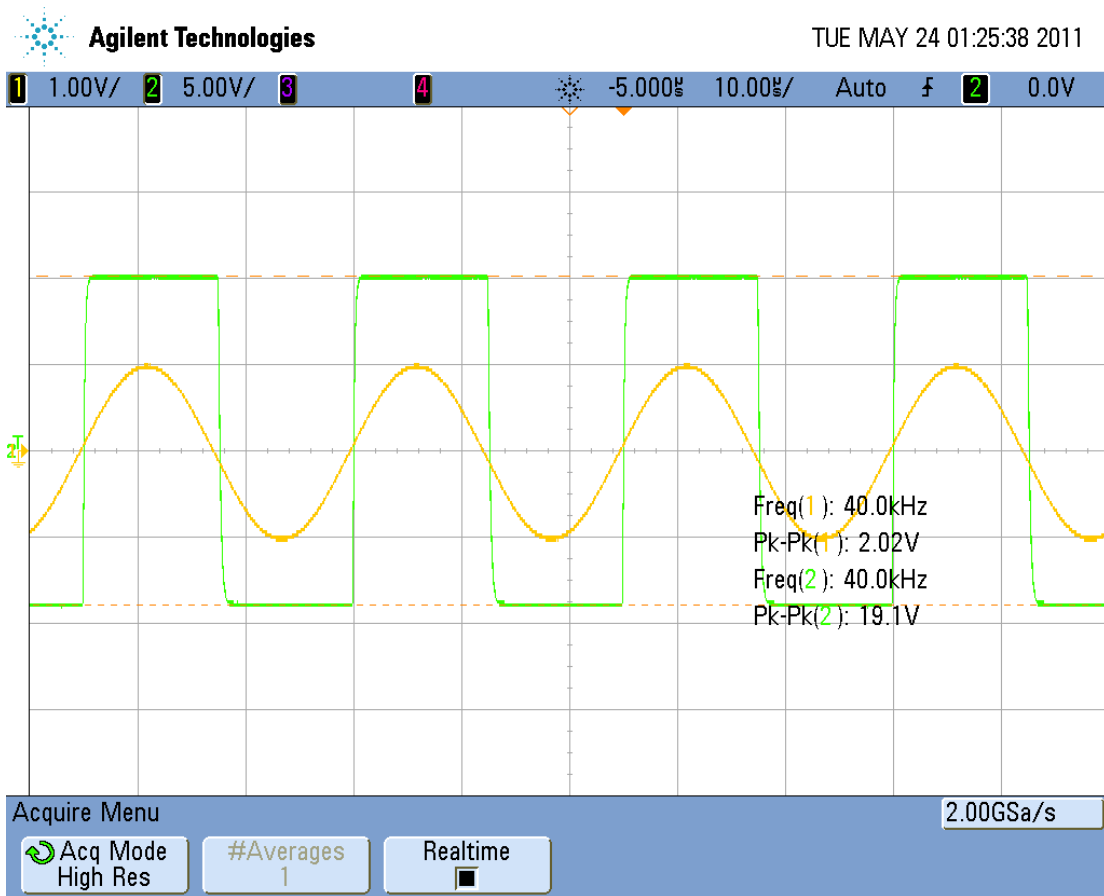
Figure 22: *Input (orange) and output (green) voltage waveforms of limiter stage*
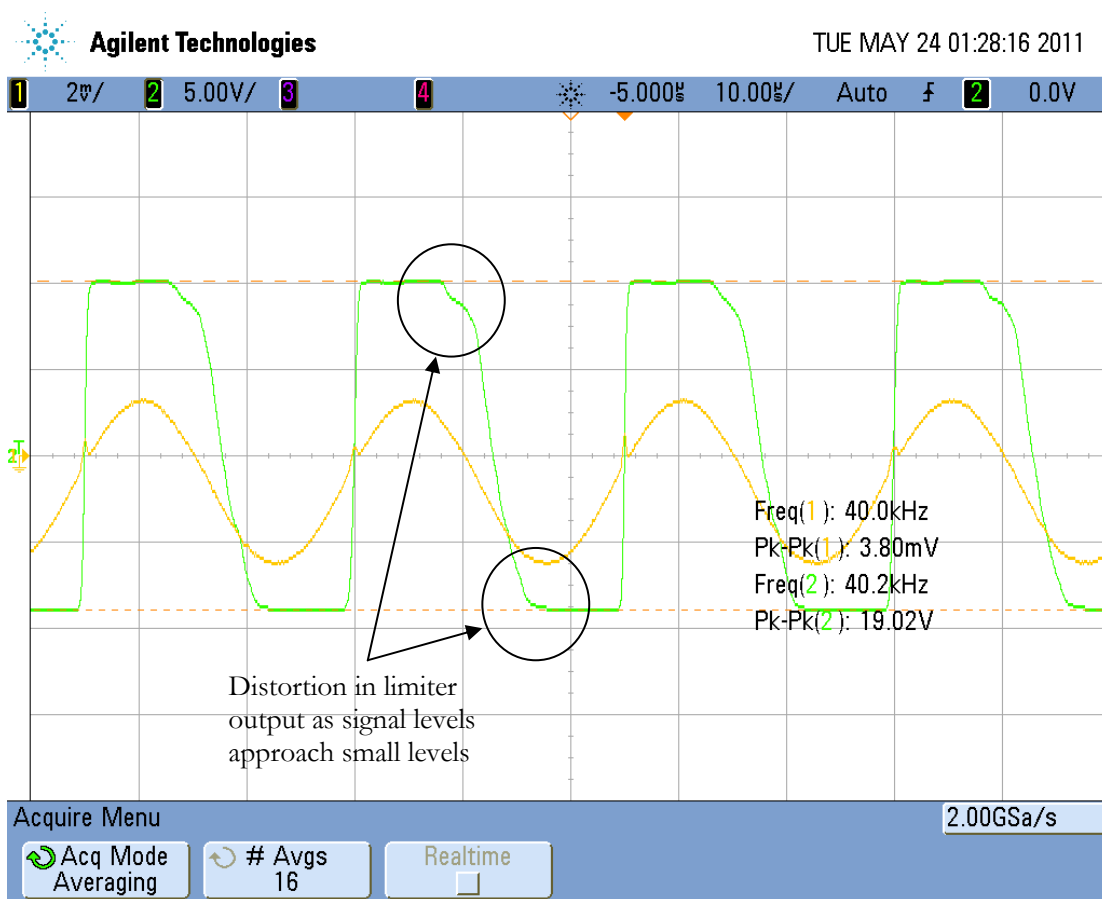*(V_{in}=2V_{p-p} @ 40kHz)*

Figure 23: *Input (orange) and output (green) voltage waveforms of limiter stage (V$_{in}$=4mV$_{p-p}$ @ 40kHz)*

5.3 Smoothing Filter Performance

The frequency response of the "smoothing" low-pass filter stage is illustrated in Figure 25 for both the simulated and experimental results. The actual cutoff frequency of the low-pass filter was about 80 kHz, which is relatively close to the desired cutoff frequency of 85 kHz.
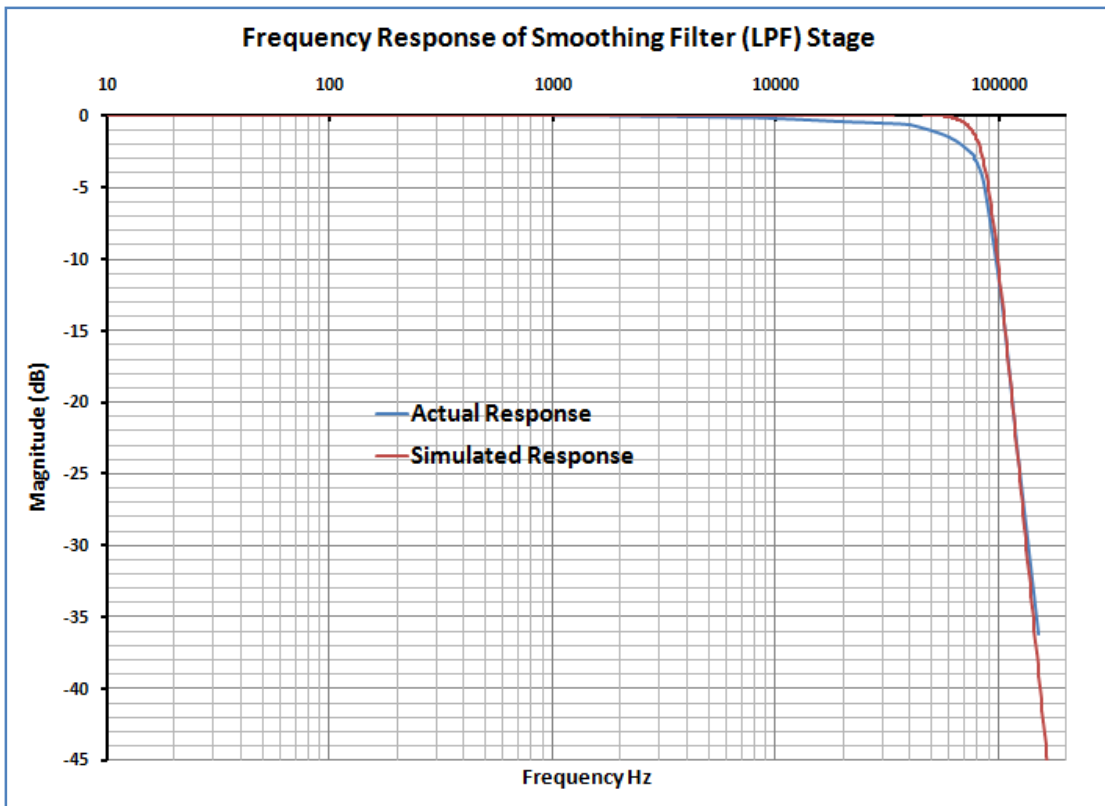
Figure 25: *Frequency response of smoothing filter (LPF)*

The input and output voltage waveforms of the smoothing filter stage are illustrated in Figure 26. The input voltage was generated using a function generator and was set to a frequency of 36 kHz with an amplitude of 10 V_{p-p} in order to replicate the square waveform output of the limiter for the minimum input frequency case. The sinusoidal output of the smoothing filter contains some distortion at this input frequency because the square wave's 3rd harmonic is around 108 kHz, which is not far enough from the cutoff frequency of 85 kHz to be completely suppressed. Plots of the input and output voltage waveforms of the smoothing filter at input frequencies of 40 kHz and

44kHz are illustrated in Figures 27 and 28, respectively. The output voltage waveforms

for these two input frequencies are less distorted because their 3rd harmonics are far
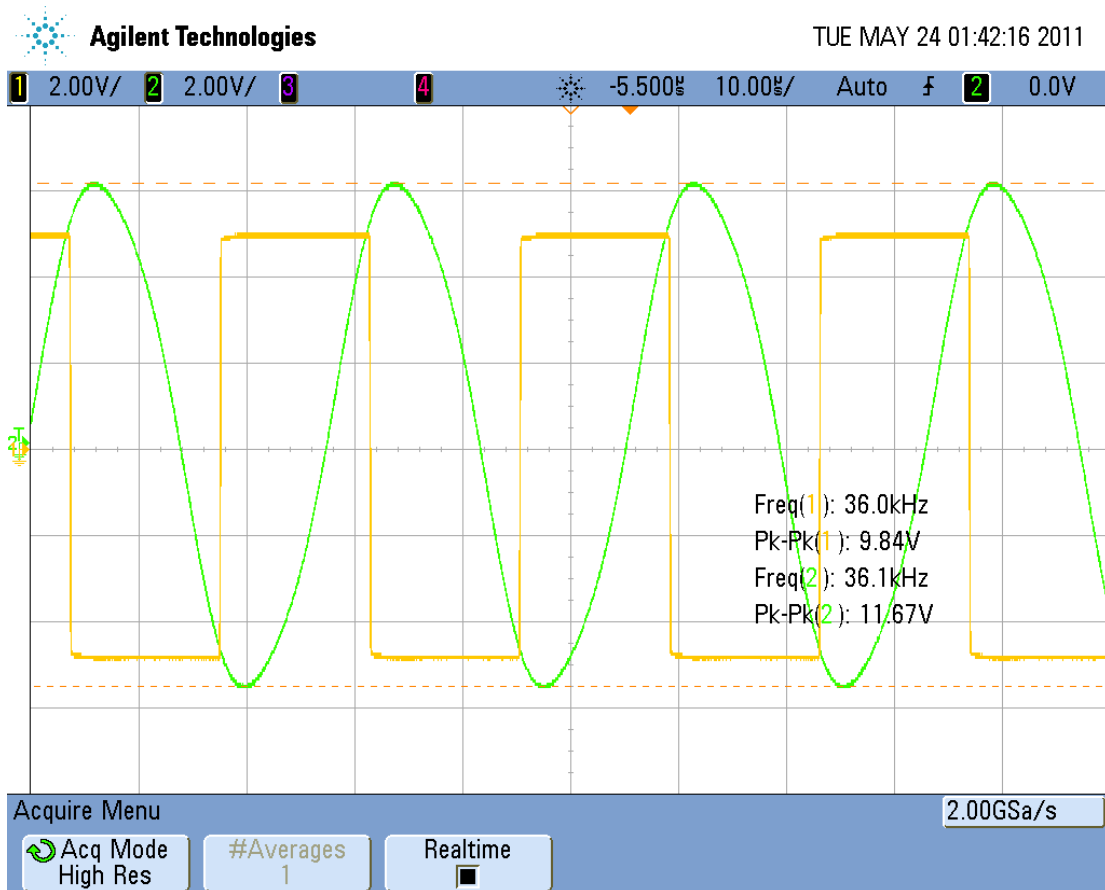
enough to be suppressed by the smoothing filter.

Figure 26: *Input (orange) and output (green) voltage waveforms of smoothing filter stage (V_{in}=10V_{p-p} @ 36kHz)*
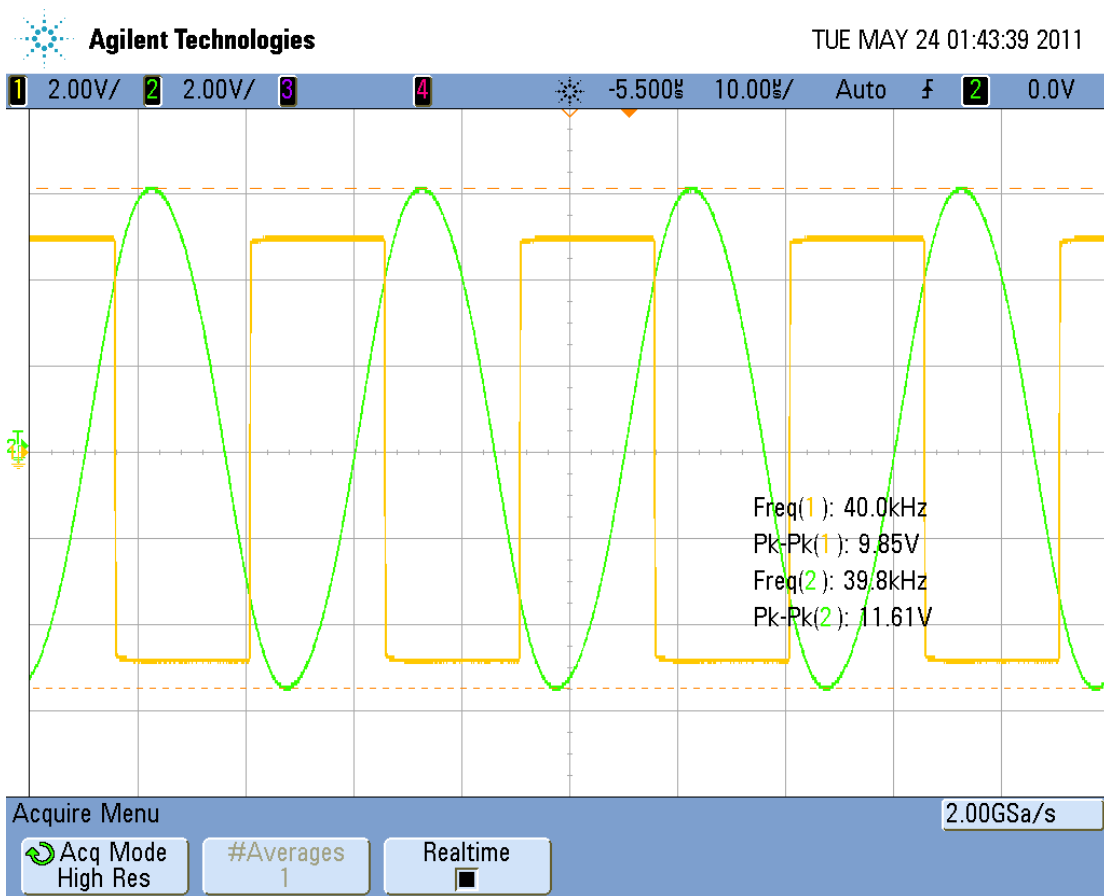
Figure 27: *Input (orange) and output (green) voltage waveforms of smoothing filter stage (V$_{in}$=10V$_{p-p}$ @ 40kHz)*
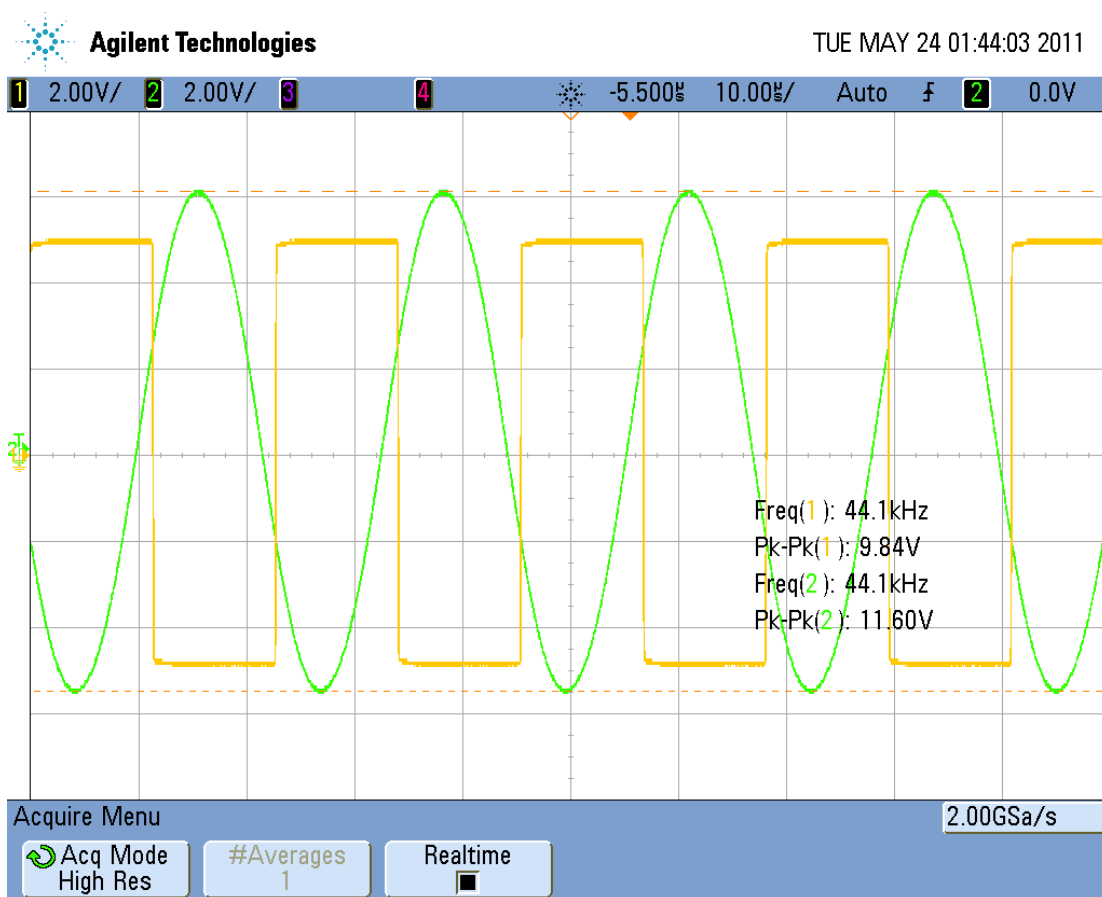
Figure 28: *Input (orange) and output (green) voltage waveforms of smoothing filter stage (V$_{in}$=10V$_{p-p}$ @ 44kHz)*

A comparison between the input voltage of the limiter and the output voltage of the smoothing filter is illustrated in Figure 29. The input signal is a sinusoidal waveform with an input voltage of 1 V$_{p-p}$ at a frequency of 36 kHz. The main difference between the two signals is the phase shift of approximately 180° and loss in amplitude from 20 V$_{p-p}$ to about 14.8 V$_{p-p}$. The phase shift occurs due to the fact that op-amps essentially act as an integrator and contain a 90° phase shift. The loss in amplitude occurs because of the attenuation experienced within the passband. This same comparison between the input voltage of the limiter and the output voltage of the smoothing filter was measured

at input frequencies of 40 kHz and 44 kHz, which are illustrated in Figures 30 and 31, respectively. When adjusting the input frequency to a higher range, the resulting output of the smoothing filter again contains little distortion compared to lower frequencies.
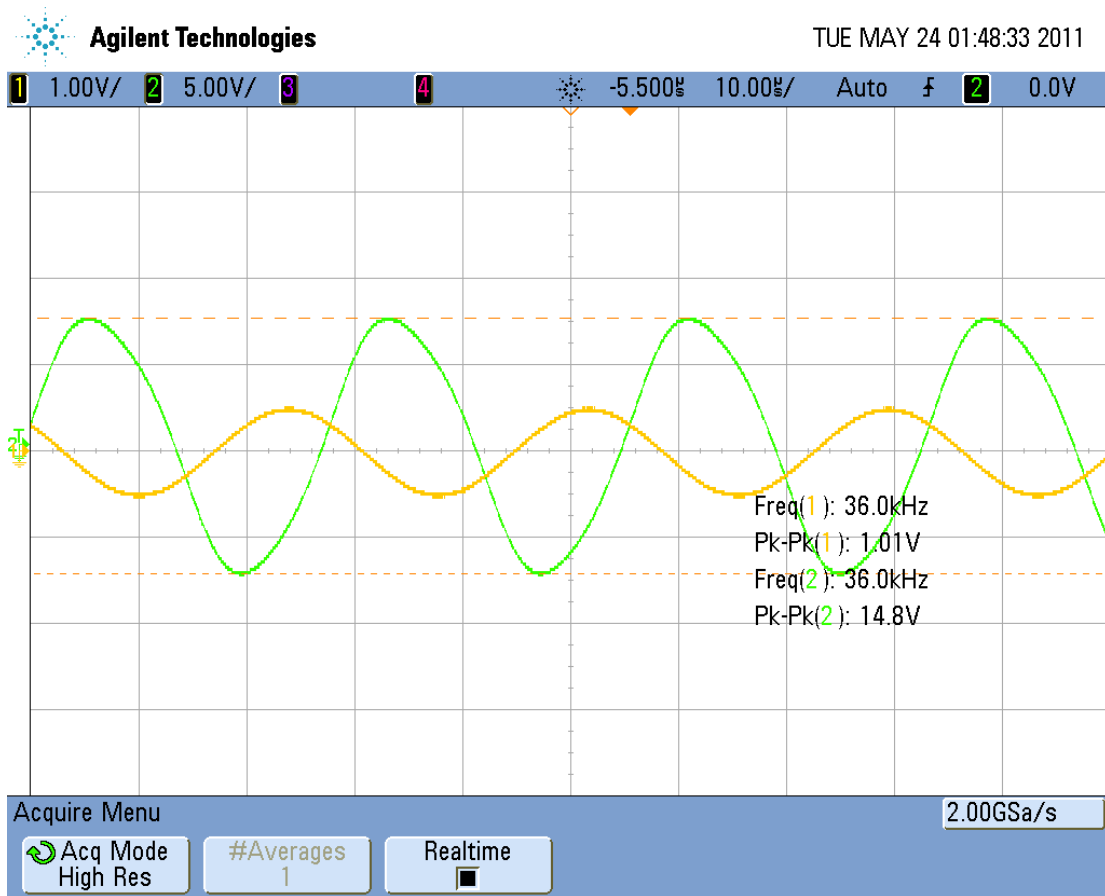

Figure 29: *Input (orange) and output (green) voltage waveforms of limiter and smoothing filter, respectively ($V_{in}=1V_{p-p}$ @ 36kHz)*
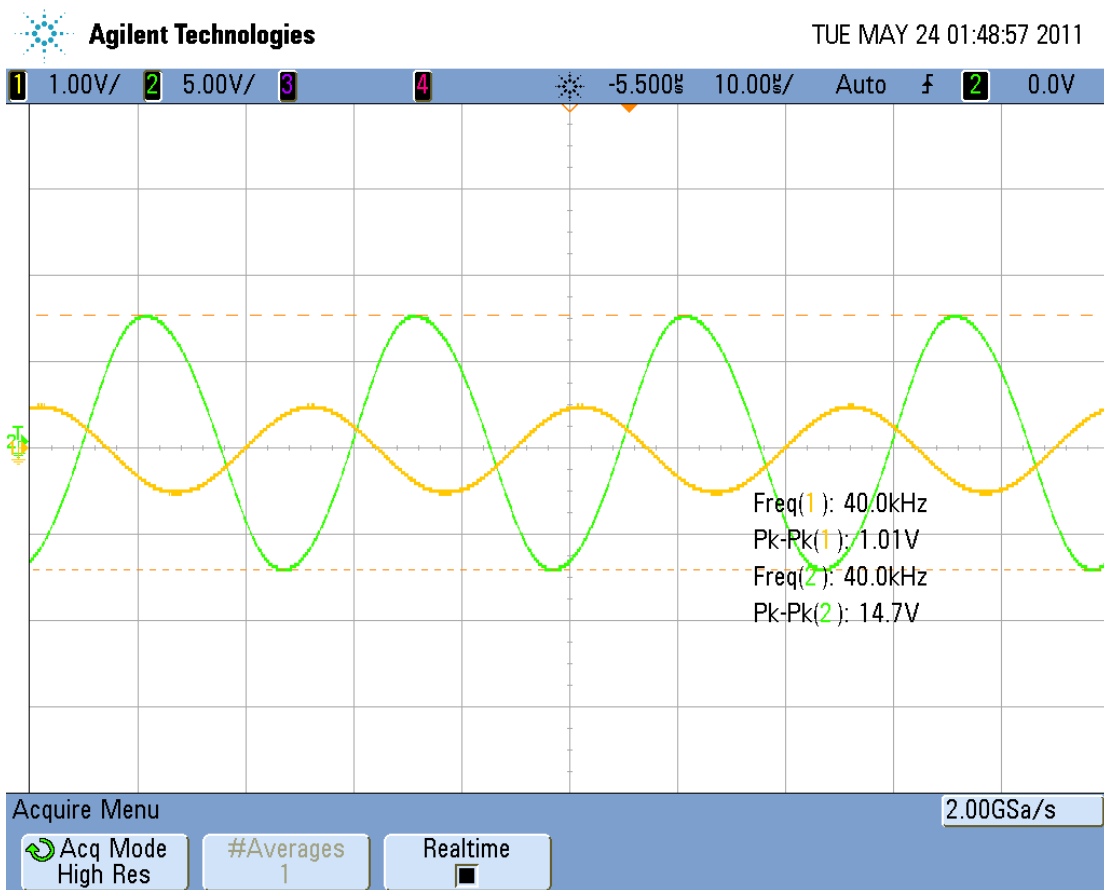
Figure 30: *Input (orange) and output (green) voltage waveforms of limiter and smoothing filter, respectively (V$_{in}$=1V$_{p-p}$ @ 40kHz)*
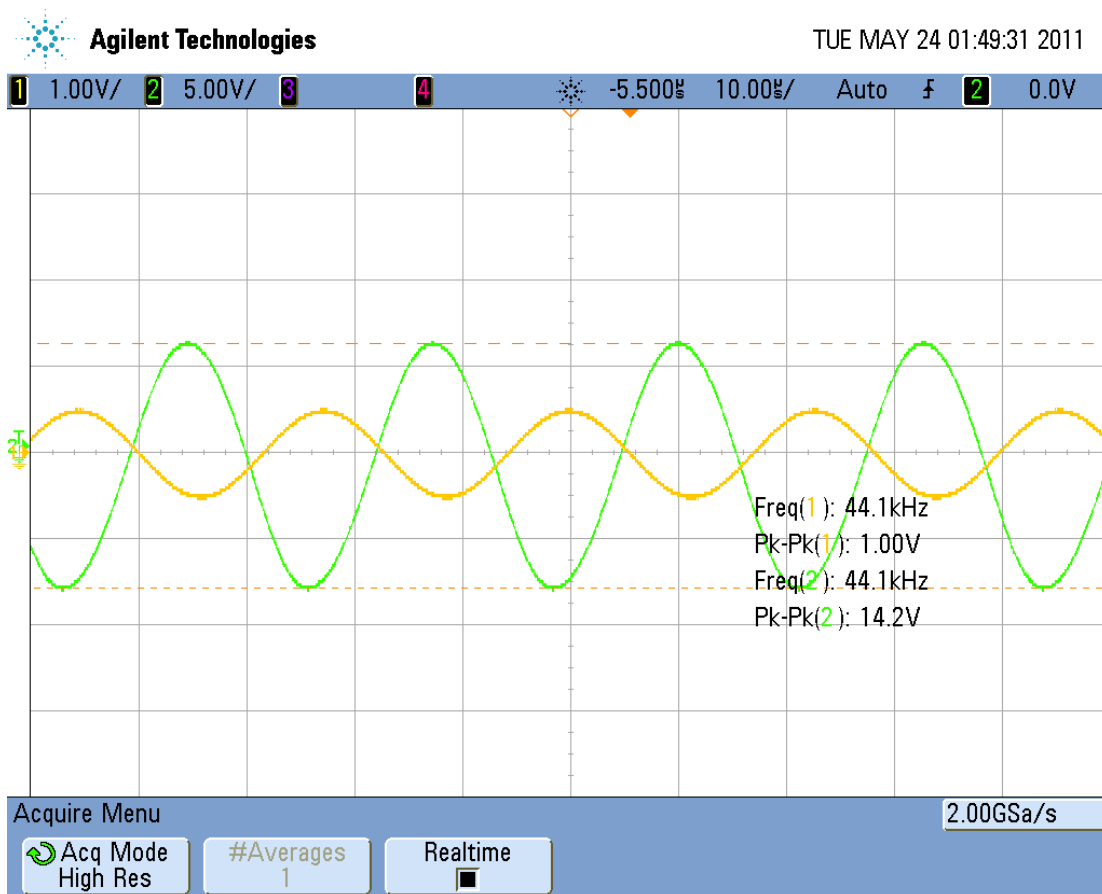
Figure 31: *Input (orange) and output (green) voltage waveforms of limiter and smoothing filter, respectively (V$_{in}$=1V$_{p-p}$ @ 44kHz)*

5.4 FM Slope Detector Performance

The frequency response of the high-pass filter that acts as an FM slope detector is illustrated in Figure 32. This response demonstrates how the measured roll-off slope is relatively linear compared to the simulated result. Therefore, better modulation is expected to occur since the relationship between the output voltage and input frequency is linear within the frequency range of interest (36 kHz to 44 kHz). Thus, a conversion from FM to AM modulation occurs.
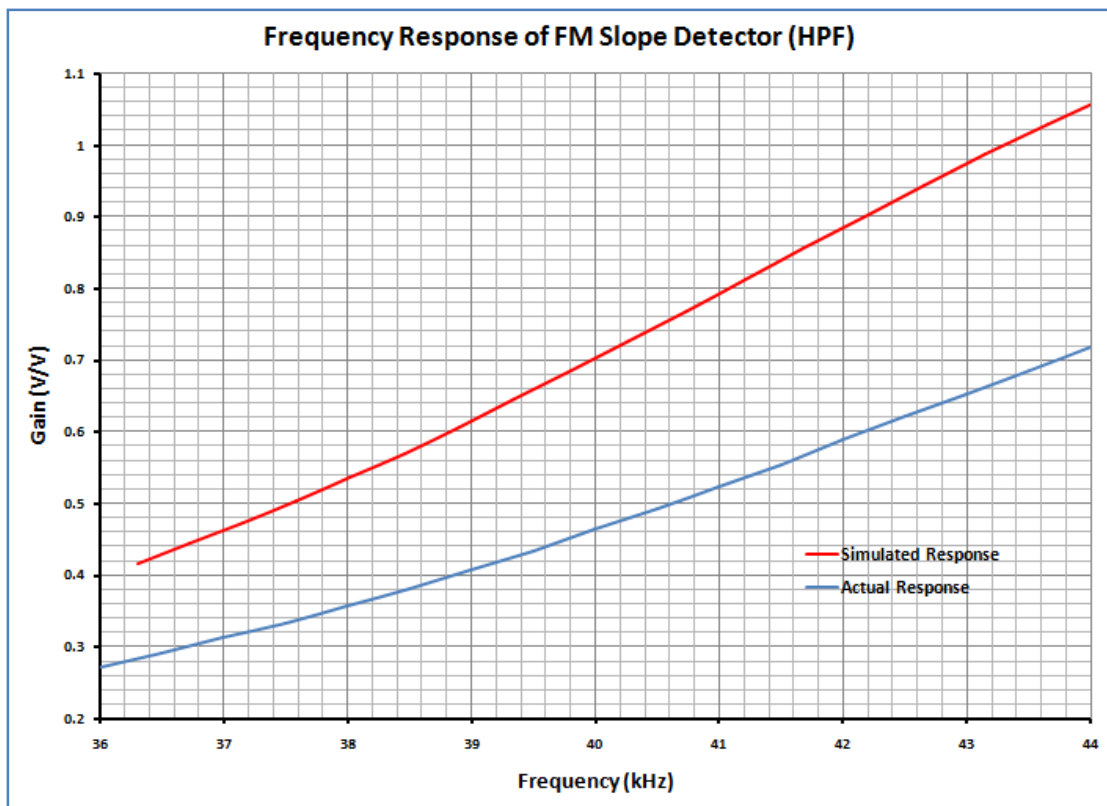
Figure 32: *Frequency response of FM slope detector (HPF)*

5.5 Envelope Detector Performance

The initial circuit configuration of the envelope detector illustrated Figure 12 contained 1N4001 diodes. With these diodes, the resulting signal contained large losses and was relatively small compared to what was expected. This occurred because the diodes were too slow, resulting in a rectified signal that contained negative excursion as illustrated in Figure 33. Once the 1N4001 diodes were replaced with faster 1N4154 diodes, the rectified signal contained very little negative excursions as shown in Figure 34.
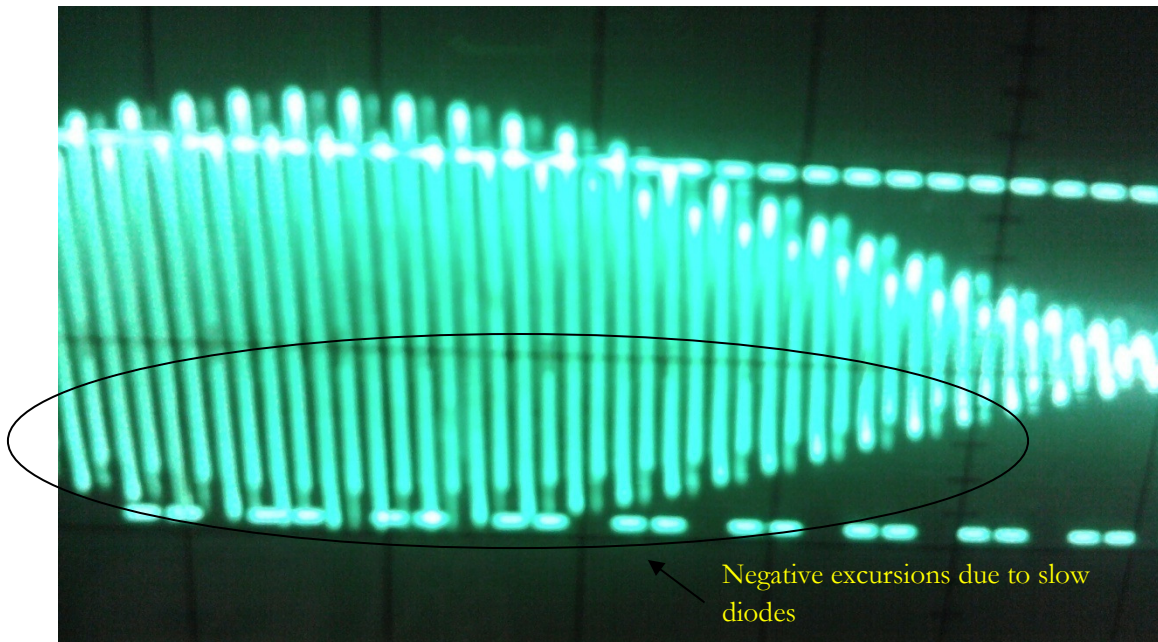
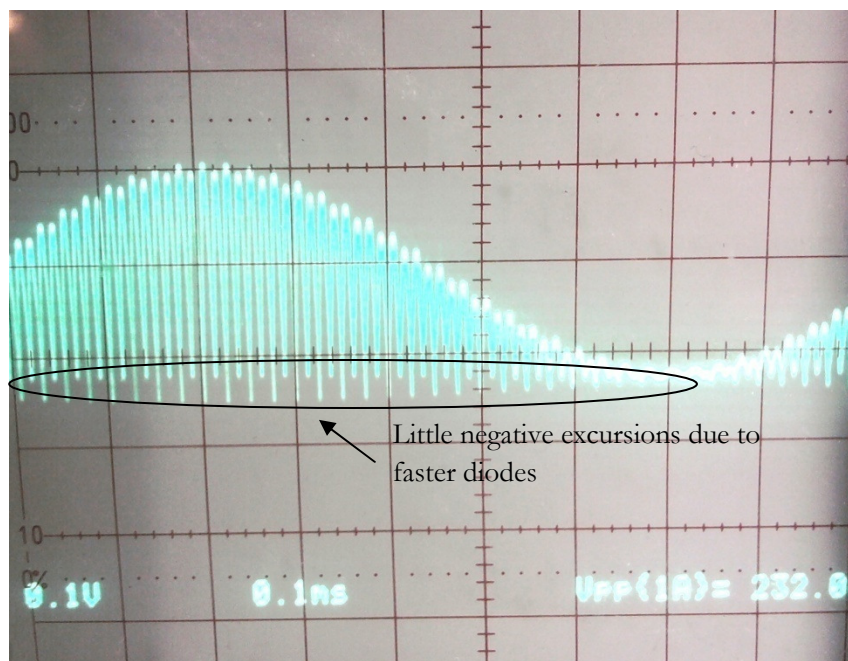**Figure 33:** *"Rectified" output voltage of envelope detector with 1N4001 diodes*

Figure 34: *Rectified output signal of envelope detector with 1N4154 diodes*

Another issue with the envelope detector was that the active low-pass filter is a 1st order, thus, high frequency noise was experienced. Therefore, an additional low-pass filter was added to remove the high frequency noise.

5.6 DC Block Performance

The frequency response of the high-pass filter used for the DC block stage is illustrated in Figure 35 for both the simulated and experimental results. The measured cutoff frequency was nearly identical to the desired 100 Hz. The high-pass filter in Figure 13 proved to help with filtering of insignificant frequencies under 100 Hz and served as an efficient DC block for the system.
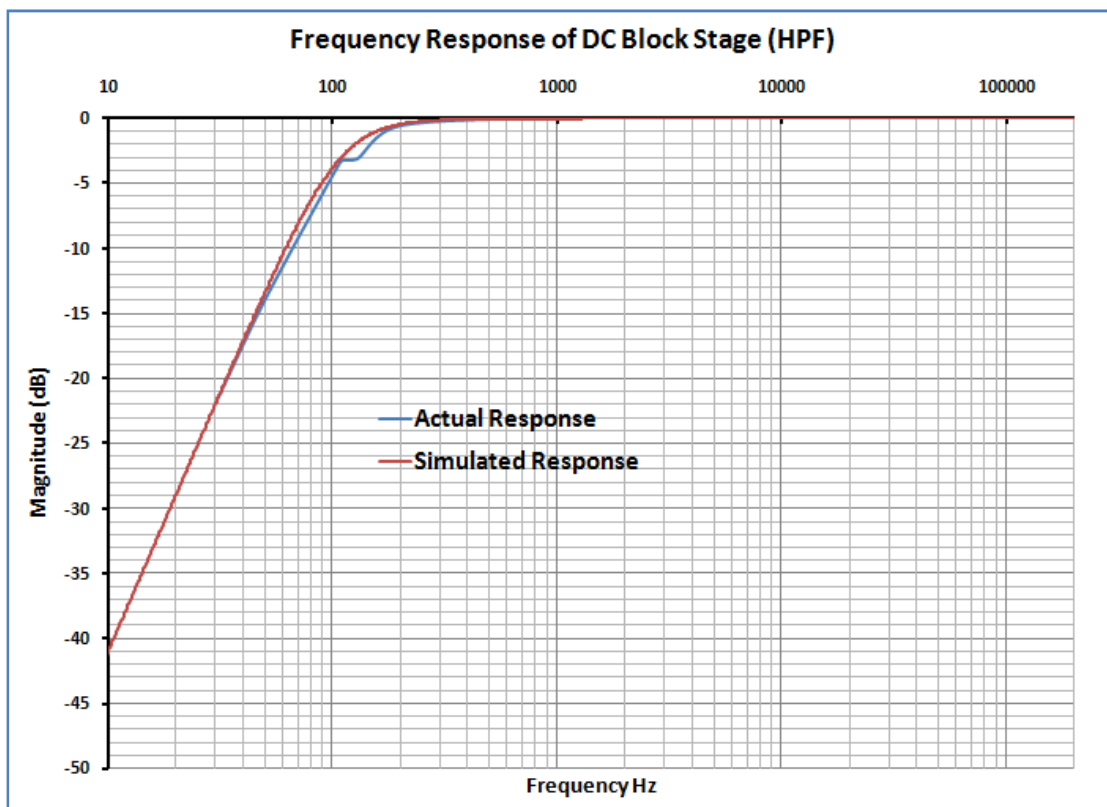
Figure 35: *Frequency response of DC block (HPF)*

5.7 Additional Filtering Stage Performance

The frequency response of the additional low-pass filter is illustrated in Figure 36 for both the simulated and experimental results. The measured cutoff frequency of 4.5kHz was relatively close to the desired cutoff frequency of 4 kHz. This circuit proved to be useful in removing the high frequency noise that was present in the envelope detector output.
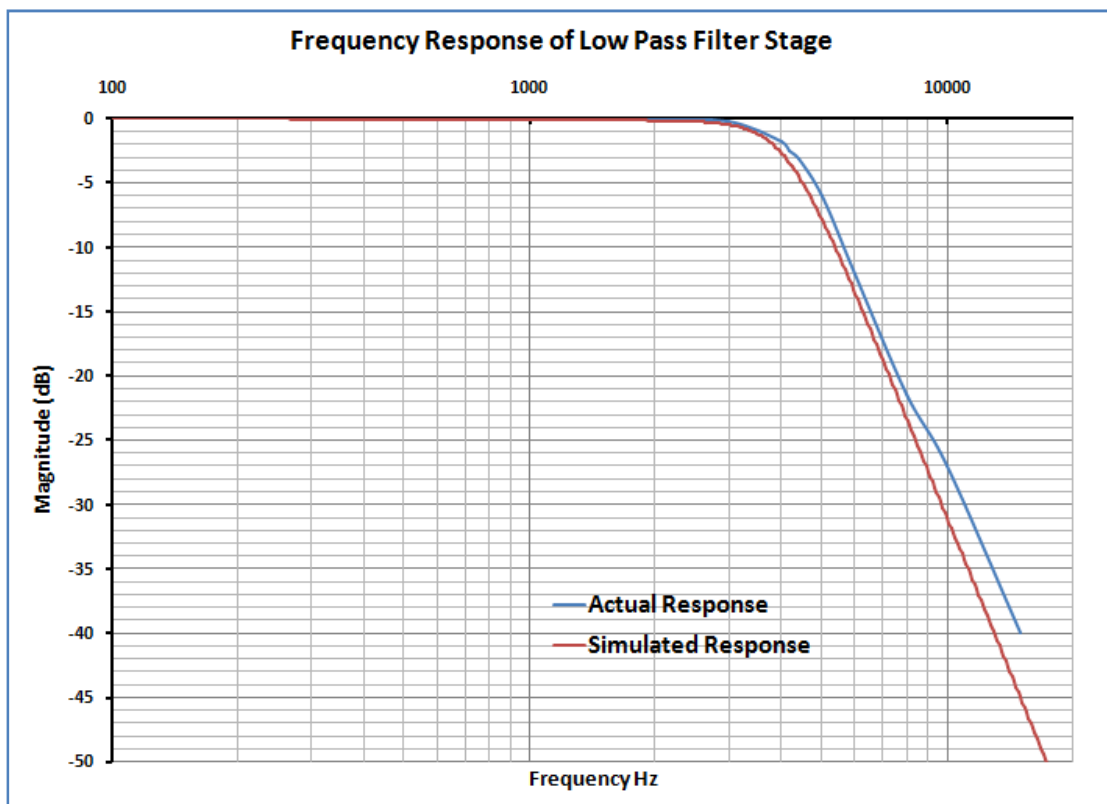
Figure 36: *Frequency response of additional low-pass filter*

5.8 AM Versus FM System Performance

The overall performance for the AM system with all circuits configured as in the block diagram in Figure 4 is illustrated in Figure 37.

Figure 37: *Plot of overall AM system performance*

The first waveform (orange) is the amplitude modulated signal generated from the function generator. A 1 kHz tone was implemented with a 1 V_{p-p} amplitude at 40 kHz carrier frequency. The second waveform (green) illustrates the received signal after being transmitted with a stationary distance of 0.5 meters between Tx and Rx UTs. The third waveform (purple) illustrates the output of the smoothing filter, which contains a

DC offset voltage. This waveform contains a significant amount of harmonics high frequencies that were not removed after the envelope detector stage. These extra harmonics are suppressed after passing through the additional low-pass filter. The result is a 1 kHz tone signal (pink) with amplitude of approximately 200 $mV_{p\text{-}p}$ that contains little noise.

The overall performance for the FM system with all circuits configured as in the block diagram in Figure 4 is illustrated in Figure 38.
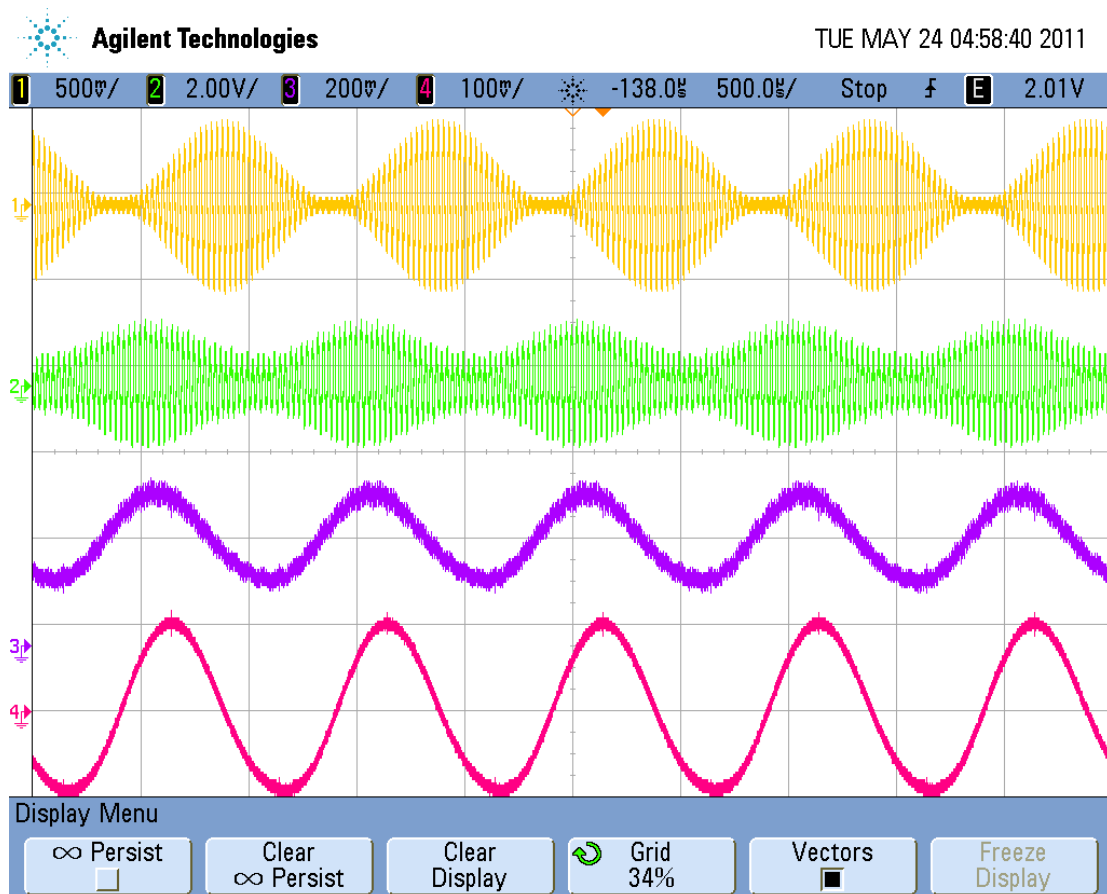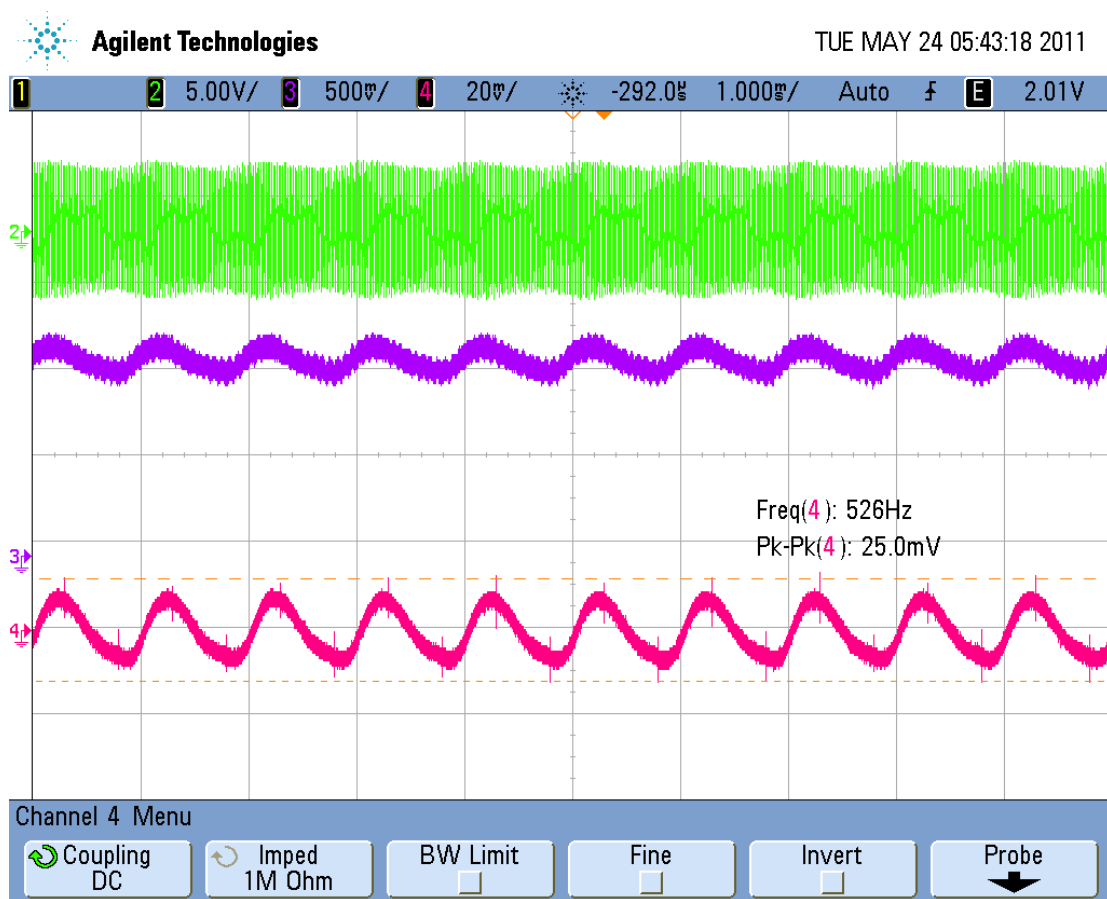

Figure 38: *Plot of overall FM system performance*

A 1 kHz tone was applied at the same distance from the function generator. The first waveform (green) is the amplitude modulated signal that was received by the Rx UT. This signal is severely under-modulated. It is not fully understood what caused this. It is assumed that the front end of the circuit (i.e. limiter or difference in UT's sensitivity within desired frequency range) is what may have caused this result. Another reason may have originated from the way that group delays affect FM signals. In air, different frequencies are adversely affected by different surrounding conditions. Ultimately, this may cause some frequencies to arrive at the receiver at later than other frequencies. This is non-ideal.

The second waveform (purple) illustrates the output of the smoothing filter, which again contains a DC offset voltage and a significant amount of harmonics at high frequencies that were not removed by the envelope detector stage. Additional low-pass filtering helped remove these harmonics as seen in the third waveform (pink), but the signal was still highly distorted due to poor front end performance.

Ideally, the FM technique should have proved to contain a better performance compared to AM, but the result did not demonstrate this. The AM case was actually contained a better demodulated signal than the FM case. Therefore, further investigation needs to go into the development of a more efficient limiter stage and alternate solutions to the group delay that may cause this performance degradation.

VI.   CONCLUSION AND RECOMMENDATIONS

The investigation into various modulation techniques for use in an ultrasonic transceiver system proved to be a productive learning curve. Various UTs were experimented with for use in this wireless system and multiple demodulation techniques proved to be useful. However, there were also some issues involving system performance that were uncovered. Even though time did not permit some of these problems experienced to be fully understood or solved, such as the FM performance degradation compared to AM, there are a handful of issues that may be investigated in the future.

Future investigation involves many aspects of the near-body ultrasonic transceiver system that were uncovered throughout this project. First, issues involving the FM performance must be more closely investigated in order to determine what techniques to avoid for future applications. Second, alternate UTs with better performance in regards to radiation patterns, power consumption, etc. may assist in a ultrasonic system that is highly feasible and efficient for near-body applications. Third, a considerate amount of research must be spent digitalizing the ultrasonic system, which is ultimately the main goal of this type of system. Therefore, digital modulation techniques, such as ASK, FSK, etc. need to be thoroughly explored to determine which have the best qualities for a low-power, low-rate, and minimally sized system. Overall, this digital system must be able to integrate with a wide variety of interfaces in order to optimize its use for various applications.

VII.   BIBLIOGRAPHY

[1] Liscano, Ramiro. *Introduction to Bluetooth Networking*. 4 May 2011. Web: <http://www.ee.ucla.edu/~lerong/ee202a/hw2/Introduction%20To%20Blue%20Tooth%20Networking.pdf>. (Page 8)

[2] OSHA. *Radiofrequency and Microwave Radiation*. 4 May 2011. Web: <http://www.osha.gov/SLTC/radiofrequencyradiation/index.html>.

[3] "Piezoelectricity." Wikipedia: The Free Encyclopedia. Wikimedia Foundation, Inc. 5 May 2011. Web: <http://en.wikipedia.org/wiki/Piezoelectricity>.

[4] PZT Application Manual. 5 May 2011. Web: <http://www.aurelienr.com/electronique/piezo/piezo.pdf>.

[5] B.P. Lathi and Zhi Ding. *Modern Digital and Analog Communication Systems*, 4th Edition. Oxford, New York: Oxford University Press, Inc., 2009. (pages 11-12)

[6] York, Bob. ECE 2C Lab#4: *Ultrasonic AM Receiver Laboratory Experiment*. University of California, Santa Barbara, 2007. 20 February 2011. Web: <http://www.ece.ucsb.edu/yuegroup/Teaching/ECE2C/Lab/Lab4.pdf>. (Pages 5-7)

[7] Prodanov, Vladimir. EE 409, Lecture 7, Slide 11: *Electrocardiogram (EGC) Amplifier, Precision Rectifiers*. California Polytechnic State University, San Luis Obispo, 2010.
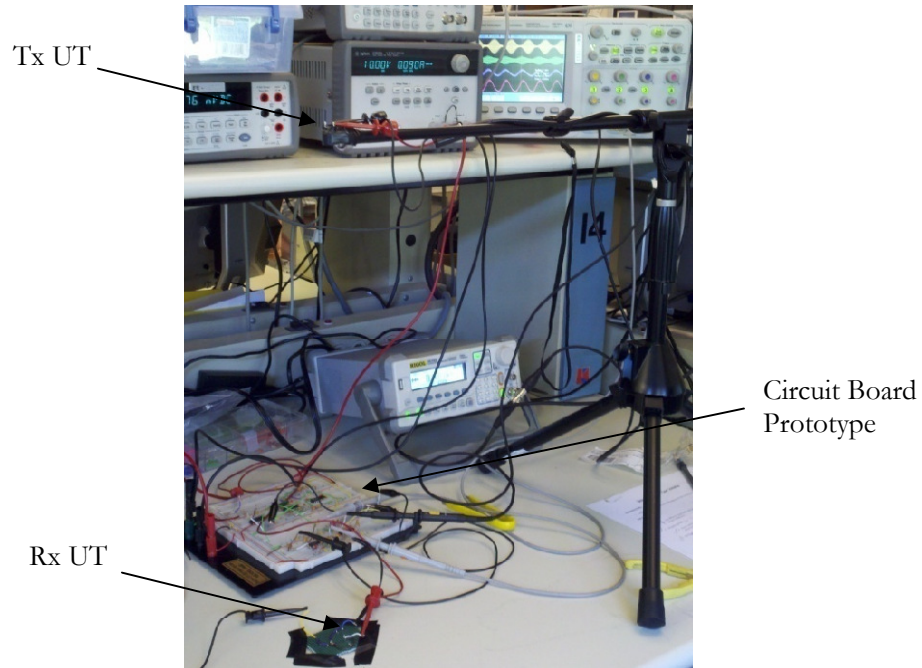
APPENDICES

A. Image of System Configuration

Figure 39: *Image of system configuration*

B. Parts List and Cost

Table 2: *Parts List and Cost*

Description	Quantity	Cost ($)
Kobitone #255-400ST12-ROX UT	1	5.24
Knowles Acoustic: SPM0404UD5 UT	1	5.00
LT1362 Quad Op-Amp IC Package	4	1.99
LM339 Quad Comparators IC Package	1	1.99
LM386 Audio Power Amp	1	1.49
LM741 General Purpose Op-Amp	2	0.60
5% Resistors	41	4.10
Potentiometer	1	0.50
10% Capacitors	29	4.93
Electrolytic Capacitor	1	0.62
1N4154 Diode	2	0.12
8 Ω Speaker	1	3.00
Condenser Microphone	1	1.88
TOTAL		**31.46**

C. Associated MATLab Code: Radiation Pattern Plotting

```
%Plot Transducer Data in a Polar Plot

theta=(pi/180)*[-90,-80,-70,-60,-50,-40,-30,-20,-10,0,...
        0,10,20,30,40,50,60,70,80,90];
pkk=[4.1,3.9,4.06,4.2,3.7,3.1,2.5,2.4,1.8,1.5];
pkk_mirror=fliplr(pkk);
rho=[pkk_mirror pkk];

polar(theta,rho,'r'); grid on
title(t1,'FontSize',13,'FontName','Calibri','FontWeight','b')
```